KLF15 Negatively Regulates Cardiac Fibrosis and SDF-1β Attenuates Cardiac Fibrosis Through KLF15 Pathway in Type 2 Diabetic Mice

Yuanyuan Tian
Jilin University First Hospital
Zhenyu Wang
Jilin University First Hospital
Xiangyu Zheng
Jilin University First Hospital
Shihuan Cheng
Jilin University First Hospital
Wenjing Song
Jilin University First Hospital
Zhe Jing
Jilin University First Hospital
Lu Cai
University of Louisville School of Medicine
Madhavi Rane
University of Louisville School of Medicine
Yuguang Zhao (zhaoyuguang@jlu.edu.cn)
Jilin University First Hospital

Original investigation

Keywords: Type 2 diabetes, Diabetic cardiomyopathy, KLF15, SDF-1β, Cardiac fibrosis, CXCR7, p38 MAPK, Cardiac function

Posted Date: November 24th, 2020

DOI: https://doi.org/10.21203/rs.3.rs-112222/v1

Abstract

Background: Diabetic cardiomyopathy (DCM) is a common complication in diabetic patients. Cardiac fibrosis is the major pathologic changes, for which the effective and safe approaches remain not available.

Methods: Wild-type mice and conditional knockout of cardiac specific *Klf15* gene (*Klf15*-cKO) mice were fed with either high fat diet (HFD, 60% kcal from fat) or normal diet (ND, 10% kcal from fat) for 3 months and then injected with streptozotocin or vehicle. Five days later mice with hyperglycemia (3 h fasting blood glucose level ≥ 250 mg/dL) were defined as type 2 diabetes (T2D). All T2D and age-matched control mice that were continually received their HFD or ND for 6 months were treated with or without SDF-1β at 5 mg/kg body-weight twice a week for 3 months. At the end of 9-month study, after cardiac functions measured, mice were euthanized, for collecting heart tissue. For the *in vitro* study, H9C2 cells were exposed to palmitate to mimic *in vivo* condition of T2D.

Results: SDF-1β treatment attenuated T2D-induced cardiac dysfunction and fibrosis and down-regulated KLF15 expression in wild type diabetic mice. The inhibitory effect of SDF-1β on cardiac fibrosis was abolished in *Klf15*-cKO/T2D mice, demonstrating the KLF15-dependence for this protection. Pre-treatment of H9C2 cells with the relevant siRNAs, followed by treatment with palmitate or SDF-1b or palmitate/SDF-1b demonstrated that SDF-1β inhibited palmitate-induced myocardial fibrosis through its receptor CXCR7 mediated activation of p38β MAPK and subsequent blockade of KLF15 down-regulation.

Conclusions: T2D-promoted cardiac fibrosis and dysfunction were prevented with SDF-1β treatment by up-regulating KLF15 expression. Conditional knockout of cardiac specific *Klf15* gene abolishes SDF-1β prevention of cardiac fibrosis but not cardiac dysfunction. The SDF-1β's anti-fibrosis effect in the heart of T2D is probably mediated through CXCR7-mediated p38β MAPK activation of KLF15 function.

1. Background

As a multifactorial disease characterized by hyperglycemia, the incidence of diabetes mellitus (DM) has been increasing and has quickly become one of the most prevalent and costly chronic diseases worldwide (1). According to the latest data, 463 million adults currently have diabetes. Unless we take action to address the epidemic, 578 million people will have diabetes by 2030. By 2045, that number will jump to a staggering 700 million (2).The continued rise is largely due to an upsurge in type 2 diabetes (T2D) and related risk factors, which include rising levels of obesity, unhealthy diets and widespread physical inactivity (2). Diabetes and elevated blood glucose are associated with an approximate doubling of cardiovascular disease (CVD) risk, and CVD is the most prevalent cause of diabetes-related morbidity and mortality (3). Diabetic cardiomyopathy (DCM) is a specific cardiomyopathy that is independent of hypertension and coronary heart disease, or any other known cardiac diseases (4). The pathogenesis of DCM will undoubtedly be multifactorial and complex, contributing to downstream structural and functional alterations in the heart, such as myocardial fibrosis and myocyte hypertrophy, which ultimately

lead to DCM and heart failure (5). Therefore, identifying mechanisms regulating myocardial fibrosis caused by T2D, can lead to identification of therapies to prevent or to inhibit progression of myocardial fibrosis, to prevent or delay the occurrence of DCM in T2D patients.

Chemokine stromal cell-derived factor (SDF-1), also known as chemokine (C-X-C motif) ligand 12 (CXCL12), regulates many essential biological processes, including cardiac and neuronal development, stem cell motility, neovascularization, angiogenesis, and tumorigenesis (6, 7). Six variants of SDF-1, including SDF-1α, β, γ, δ, ε, and θ have been identified to date (8, 9). SDF-1α and SDF-1β have identical amino acid sequences except for the presence of 4 additional amino acids at the carboxy terminus of SDF-1β (10, 11). SDF-1α and SDF-1β are mostly involved in cardiovascular diseases (12, 13). SDF-1 regulates many essential biological processes, predominantly through chemokine receptor CXCR4 (7, 14). In 2005, Balabanian *et al* revealed that SDF-1 can bind to the second chemokine receptor CXCR7 with a 10-fold higher affinity than CXCR4 (15). In humans, CXCR7 is expressed in heart, brain, endothelium, kidney, and tumor cells (16, 17). Previous studies have shown that SDF-1/CXCR4 signaling has a protective effect on the survival of hypoxic cardiomyocytes after myocardial infarction and ischemia/reperfusion injury (18–20). However, recent studies have implicated that CXCR7 and CXCR4 mediate distinct functions and can also play an important role in mediating cell survival or the anti-apoptotic effect of SDF-1 (14). In our previous study, we have demonstrated that SDF-1β protects against cardiac apoptosis *via* CXCR7 in T2D animal model (21). Currently, the role of SDF-1β in modulating myocardial fibrosis in T2D mice is not known. Therefore, research examining the role of SDF-1β in delaying or preventing myocardial fibrosis in T2D mice along with identifying the mechanisms underlying these effects is necessary.

Krüppel-like factors (KLFs) as a subfamily of the zinc-finger class of DNA binding transcriptional regulators (22), played diverse roles in the differentiation and development of various mammalian cells, such as regulating gene expression, growth, and differentiation (23). The transcriptional factor KLF15 is widely expressed, with abundant expression in liver, kidney, heart and skeletal muscle. Immunohistochemistry revealed that KLF15 protein is located in interstitial fibroblasts of heart and skeletal muscle and in potentially fibrogenic cells such as the mesangial cells in the kidneys or stellate cells in the liver, therefore, it is reasonable to postulate that KLF15 may be involved in the fibrogenesis in these organs (24). Under pathophysiological conditions, KLF15 repressed expression of connective tissue growth factor (CTGF), tissue growth factor-β (TGF-β), and myocardin-related transcription factor-A in cardiac fibroblasts, leading to the alleviation of cardiac fibrosis and improvement of cardiac function. Accordingly, a low expression of KLF15 could promote fibrotic remodeling during pathological left ventricular hypertrophy (LVH) (25, 26). In experimental models, Fisch *et.al* have demonstrated KLF15 expression in the heart and that KLF15 functioned as a transcriptional repressor in pathological cardiac hypertrophy through inhibition of the myocyte enhancer factor 2 (MEF2) and GATA binding protein 4 (GATA4) transcriptional pathway (27). Wang *et.al* also demonstrated that adenoviral overexpression of KLF15 significantly inhibited the basic expression of CTGF in neonatal rat ventricular fibroblasts and as well as CTGF expression induced by TGF-β1. After ligating the aorta of *Klf15* knockout mice, the expression of CTGF in the heart increased and the degree of cardiac fibrosis increased (26). In 2017, for

the first time, a human study indicated the potential importance of KLF15 in promoting cardiopathological changes in the patients with T2D. In this study, they associated *Klf15* SNP rs9838915 A allele with increased left ventricular (LV) mass in patients with T2D and these findings were replicated in a large independent cohort (28). These studies promoted us to question whether KLF15 plays an important role in the left ventricular hypertrophy of patients with T2D (29). In our previous study, we have demonstrated that SDF-1β protects against cardiac apoptosis *via* CXCR7 in T2D animal model (21). Therefore, in the current study we hypothesize that SDF-1β could alleviate T2D-induced myocardial fibrosis in a KLF15 dependent manner. In the following research, we examined the protective effect of SDF-1β on T2D-induced myocardial fibrosis and systematically investigated the function of KLF15 in this process.

Leenders *et.al* revealed that TGF-β1 down-regulated KLF15 expression in cardiomyocytes in a p38 mitogen activated protein kinase (p38 MAPK) dependent manner and promoted ventricular hypertrophy (30). However, they did not examine the involvement of a precise p38 MAPK isoform. There are four members of the p38 MAPK family in mammals: α, β, γ and δ (31). Of the four known isoforms of p38 MAPKs, p38α and p38β are abundant in cardiomyocytes, while no expression of p38γ and p38δ isoforms was detected in the heart (32). In contrast, we have demonstrated that p38β MAPK activation was required for SDF-1β mediated cardiac protection from palmitate-induced cardiac cell apoptosis (21). In the current study, we evaluated the protective role of SDF-1β on T2D-induced myocardial fibrosis. Moreover, we also examined whether p38 MAPK mediated the protective effects of SDF-1β and if so, which isoform of p38 MAPK was involved in this process.

2. Materials And Methods

Cell culture

Embryonic rat heart derived H9C2 cells, purchased from ATCC (CRL-1446, Manassas, VA), were maintained in the conditions as instructed by ATCC. H9C2 cells were exposed to palmitate at 62.5 μM for 15 h, with SDF-1β co-treatment at 100 nM, and some of these cultures were pre-treated with siRNAs based on experimental needs. Palmitate (Sigma Aldrich, St. Louis, MO) was dissolved in 50% ethanol, heated at 70 °C for 2 min, and then added to 2% fatty acid free bovine serum albumin (BSA, Sigma-Aldrich) in medium as stock solution (2.5 mM). Before use, the stock palmitate solution was gently rotated for 1 h at 37 °C and further diluted to the required concentrations for treatment. SDF-1β, prepared as in our previous study (7, 33), was dissolved in phosphate buffered saline (PBS) to the required concentrations.

siRNAs transfection

siRNAs specific for rat p38β (Silencer® Select siRNA ID: s236087), p38α (Silencer® Select siRNA ID: s135447), CXCR7 (Silencer® Select siRNA ID: s136443), CXCR4 (Silencer® Select siRNA ID: s133527) and KLF15 (Silencer® Select siRNA ID: s137039) along with their parallel Silencer® Select negative control siRNAs (Thermo Fisher Scientific) were transfected into H9C2 cells for 48 h by transfection

reagent. Following which cells were co-treatment with SDF-1β at 100 nM and palmitate at 62.5 μM for 15 h. Transfection efficiency was assessed by ELISA kit and western blot analysis for the target genes or proteins.

Recombinant adenovirus infection

Rat KLF15 (Accession no. AAH89782.1) cloned into adenovirus vector (pAdenoMCMV-EGFP-P2A-3FLAG) were constructed by Obio Technology (Shanghai, China) (34). Adenoviral infection was performed on H9C2 cells at multiplicity of infection (MOI) of 50 for 48 hours (> 90% infection efficiency as assessed by GFP signal) (35).

Animal models

All animal protocols were approved by the Animal Ethics Committee of Jilin University. Eight-week-old male C57BL/6J mice (Weitonglihua, Beijing, China) and conditional knockout of cardiac specific *Klf15* gene (*Klf15*-cKO) mice (VivoCure, Beijing, China) were acclimated in an air-conditioned room at 22 °C with a 12 h light / dark cycle and fed with standard rodent chow and tap water. Mice were fed with either high fat diet (HFD, 60%kcal from fat, No. 12492, Research Diets, New Brunswick, NJ) or normal diet (ND, 10% kcal from fat, No. 12450B, Research Diets) for 3 months to induce insulin resistance. These insulin resistant mice were injected with a single dose of STZ (freshly dissolved in 0.1 M sodium citrate (pH 4.5), Sigma Aldrich, St. Louis, MO) at 100 mg/kg body weight to induce partial insulin deficiency. Five days after STZ injection, mice with hyperglycemia (3 h fasting blood glucose levels ≥ 250 mg/dl) were defined as diabetic. After diabetes onset, mice were divided into eight groups: Control (Ctrl, n = 6), SDF-1β (n = 6), Type 2 Diabetes (T2D, n = 7), T2D plus SDF-1β (T2D/SDF, n = 7), *Klf15*-cKO (n = 6), *Klf15*-cKO plus T2D (*Klf15*-cKO/T2D, n = 7), *Klf15*-cKO plus T2D plus SDF-1β (*Klf15*-cKO/T2D/SDF-1β, n = 7), *Klf15*-cKO plus SDF-1β (*Klf15*-cKO/SDF-1β, n = 7). At baseline, *Klf15*-cKO mice are viable and have mild pathologic remodeling of the heart (mild LVH with preserved systolic function). However, after T2D onset, *Klf15*-cKO mice develop a severe cardiomyopathy characterized by LV dysfunction, cavity dilation with attenuated wall thickening. These pathologic changes were associated with augmented cardiac mass (Table 1). SDF-1β was given by tail vein at 5 mg/kg body-weight twice a week (Tuesday and Friday) for 3 months. The dose of SDF-1β used in the present study was based on our previous study. The control mice were given the same volume of vehicle (1% dimethyl sulfoxide diluted with PBS). All T2D and age-matched control mice continually received their HFD or ND for an additional 3 months. After 3 months of SDF-1β or vehicle treatment, their cardiac function was measured, after which animals were euthanized and heart tissues were collected.

Table 1
Klf15-cKO cardiac function data

	Ctrl	T2D	T2D /SDF-1β	SDF-1β	KLF15-cKO	KLF15-cKO /T2D	KLF15-cKO /T2D /SDF-1β	KLF15-cKO /SDF-1β
IVS; d (mm)	0.61 ± 0.02	0.57 ± 0.02*	0.60 ± 0.03	0.62 ± 0.02	0.58 ± 0.02*	0.55 ± 0.03$^{\#\$}$	0.58 ± 0.03$^{\&}$	0.60 ± 0.02
LVID; d (mm)	3.79 ± 0.04	3.91 ± 0.05*	3.84 ± 0.06$^{\#}$	3.81 ± 0.06	3.89 ± 0.04*	4.03 ± 0.07$^{\#\$}$	3.94 ± 0.07$^{\&}$	3.94 ± 0.05
LVPW; d (mm)	0.79 ± 0.02	0.70 ± 0.03*	0.75 ± 0.03$^{*\#}$	0.77 ± 0.03	0.72 ± 0.02*	0.63 ± 0.04$^{\#\$}$	0.67 ± 0.04$^{\$}$	0.73 ± 0.02
IVS; s (mm)	1.07 ± 0.02	0.95 ± 0.03*	1.01 ± 0.03$^{*\#}$	1.06 ± 0.02	1.01 ± 0.03$^{*\#}$	0.84 ± 0.05$^{\#\$}$	0.93 ± 0.04$^{\$\&}$	1.03 ± 0.03
LVID; s (mm)	1.92 ± 0.09	2.39 ± 0.11*	2.03 ± 0.12$^{\#}$	1.94 ± 0.08	2.27 ± 0.13*	2.53 ± 0.14$^{\#\$}$	2.41 ± 0.09$^{\$\&}$	2.15 ± 0.09$^{\$}$
LVPW; s (mm)	1.33 ± 0.02	1.12 ± 0.03*	1.24 ± 0.03$^{*\#}$	1.31 ± 0.04	1.21 ± 0.03*	1.02 ± 0.05$^{\#\$}$	1.11 ± 0.04$^{\$\&}$	1.24 ± 0.05
LV Vol; d (mm)	61.82 ± 1.38	67.65 ± 1.74*	63.01 ± 1.53$^{\#}$	60.91 ± 1.64	65.91 ± 1.24*	72.11 ± 2.09$^{\#\$}$	69.17 ± 2.01$^{\$}$	70.26 ± 1.65$^{\$}$
LV Vol; s (mm)	12.17 ± 1.25	21.12 ± 1.53*	15.77 ± 1.43$^{*\#}$	13.02 ± 1.39	18.37 ± 1.47*	28.12 ± 1.93$^{\#\$}$	24.06 ± 1.75$^{\$\&}$	17.14 ± 1.69
%EF	78.85 ± 2.93	63.22 ± 3.35*	69.46 ± 3.73$^{*\#}$	76.91 ± 3.09	68.27 ± 3.25*	51.57 ± 3.87$^{\#\$}$	62.19 ± 3.54$^{\$\&}$	73.27 ± 3.18$^{\$}$
% FS	49.06 ± 2.81	37.91 ± 2.86*	42.05 ± 3.01$^{*\#}$	50.51 ± 3.13	40.83 ± 3.26*	29.91 ± 3.54$^{\#\$}$	35.53 ± 2.97$^{\$\&}$	42.09 ± 3.83
LV Mass (mg)	84.23 ± 2.05	82.01 ± 3.41	82.87 ± 2.53	83.25 ± 2.43	84.05 ± 2.73	82.41 ± 3.27	82.93 ± 2.96	83.71 ± 3.03

Abbreviations: EF, ejection fraction; FS, fractional shortening; IVS, interventricular septum; LV mass, left ventricular mass; LVID;d, left ventricular internal diastolic diameter; LVID;s, left ventricular internal systolic diameter; LVPW, left ventricular posterior wall; LV vol;d, left ventricular end diastolic volume; LV vol;s, left ventricular end systolic volume. Data are presented as means ± SD (n = 6 at least in each group). *P□0.05 vs. Ctrl group; $^{\#}$P□0.05 vs. T2D group; $^{\$}$P□0.05 vs. *Klf15*-cKO group; $^{\&}$P□0.05 vs. *Klf*15-cKO/T2D group.

Echocardiography

Transthoracic echocardiography was measured by a Vevo 770 ultrasound system (Visualsonics, Toronto, Canada) equipped with a high frequency ultrasound probe (RMV-707B) as described previously (36). Mice were anesthetized with intraperitoneal injection of 1.2% Avertin (Sigma, St. Louis, MO) and placed in the supine position on a temperature-controlled platform. The chest hair was removed with a depilatory to reduce ultrasound attenuation. The images were recorded in parasternal long-axis and short-axis views. The LV wall thicknesses and dimensions were measured in parasternal short axis M-mode images. At the same time, the ejection fraction (EF), fractional shortening (FS), and LV mass were calculated using Vevo770 software. The data were averaged over 10 cardiac cycles.

Western blotting

The cardiac tissues were homogenized in lysis buffer and proteins were collected by centrifuging at 12,000 × g at 4 °C (37). Western blots were performed according to our previous studies (37). Briefly, the proteins were separated on 10% SDS-PAGE gels, and then were transferred to a nitrocellulose membrane. The membrane was blocked with a 5% non-fat dried milk for 1 h and incubated overnight at 4 °C with the following antibodies: anti-phospho-p38 MAPK (Thr180/Tyr182), anti-p38 MAPK and anti-p38α MAPK (1:1000, Cell Signaling, Beverly, MA, USA), anti-CTGF and anti-p38β MAPK (1:1000, Santa Cruz Biotechnology, Santa Cruz, CA, USA), anti-CXCR7, anti-TGF-β1 and anti-Fibronectin (1:1000, Proteintech, Rosemont, IL, USA), anti-KLF15, anti-Collagen I and anti-CXCR4 (1:1000, Abcam, Cambridge, MA, USA) respectively were prepared in 5% milk in Tris-buffered saline (pH 7.2) containing 0.05% Tween 20 (TBST) solution. After removal of unbound antibodies using TBST, membranes were incubated with the secondary antibody for 1 h at room temperature. Antigen-antibody complexes were visualized using an enhanced chemiluminescence detection kit (Thermo Scientific, Barrington, IL, USA). In order to determine loading, blots were stripped using stripping buffer (Sigma Aldrich, St. Louis, MO, USA) and reprobed for β-actin as loading control of total protein. Histone was used as loading control of nuclei proteins. Quantitative densitometry was performed on the identified bands using a computer-based measurement system, as employed in previous studies (37).

Statistical analysis

Data were collected from the repeated experiments at least three times for *in vitro* studies and six animals at least for *in vivo* study and were presented as mean ± SD. One-way analysis of variance (ANOVA) was used to determine whether differences exist and if so, a post *hoc* Tukey's test was used for analysis of the difference between groups, with Origin 7.5 laboratory data analysis and graphing software. Statistical significance was considered as $p < 0.05$.

3. Results

3.1 SDF-1β inhibited myocardial fibrosis via its receptor CXCR7 activation and by p38β MAPK-mediated KLF15 up-regulation in H9C2 cells

For the *in vitro* study, embryonic rat heart derived H9C2 cells were exposed to palmitate at 62.5 μM as our previous study (21). Exposure to palmitate induced significant KLF15 down-regulation and significant CTGF up-regulation in H9C2 cells (Fig. 1A). The effect of SDF-1β at 100 nM (21) on palmitate-induced fibrosis was also examined in H9C2 cells (Fig. 1A). SDF-1β significantly prevented palmitate induced KLF15 down-regulation as well as CTGF up-regulation in H9C2 cells (Fig. 1A). Furthermore, to explore the direct role of KLF15 in mediating SDF-1β's protective role on palmitate-induced H9C2 cells fibrosis, H9C2 cells were transfected with control siRNA or KLF15 siRNA followed by co-treatment with SDF-1β at 100 nM and palmitate at 62.5 μM for 15 h. Cell lysates were immunoblotted with anti-KLF15, anti-CTGF and anti-β-actin antibodies. Figure 1B illustrated successful down-regulation of KLF15 in KLF15 siRNA transfected cells but not in control siRNA transfected cells. Palmitate induced CTGF expression was inhibited in the presence of SDF-1β in control siRNA treated H9C2 cells but not in KLF15 siRNA transfected H9C2 cells (Fig. 1B). To directly examine the role of KLF15 in modulating palmitate-induced CTGF expression, H9C2 cells were treated with KLF15 recombinant adenovirus (rAV) or control rAV. KLF15 rAV over-expression in H9C2 cells was documented by Western-blot, KLF15 expression was markedly increased in KLF15 rAV treated cells but not in control rAV treated cells (Fig. 1C). KLF15 rAV treatment significantly inhibited palmitate-induced CTGF up-regulation (Fig. 1C).

In our previous study, we demonstrated that SDF-1β protected against palmitate-induced cardiac apoptosis *via* CXCR7-mediated p38β MAPK activation (21). Therefore, CXCR7 siRNA and p38β MAPK siRNA were used respectively to define the specific role of CXCR7 and p38β MAPK on SDF-1β's protective effect against palmitate-induced cardiac fibrosis (Fig. 2). CXCR7siRNA or control siRNA were transfected into H9C2 cells for 48 h followed by treatment with palmitate and/or SDF-1β followed by immunoblotting with appropriate antibodies. Figure 2A demonstrated efficient silencing of CXCR7 expression in H9C2 cells in CXCR7 siRNA transfected but not in control siRNA transfected H9C2 cells. Silencing CXCR7 expression, but not control siRNA, abolished SDF-1β protection from palmitate-induced myocardial fibrosis, as measured by the expression of KLF15 and CTGF (Fig. 2A). Moreover, silencing p38β MAPK expression (Fig. 2B), but not control siRNA, completely abolished the protective effect of SDF-1β on palmitate-induced myocardial fibrosis, as measured by the expression of KLF15 and CTGF (Fig. 2B). Similar studies were carried out using CXCR4 siRNA and p38α MAPK siRNA, however, neither CXCR4 siRNA nor p38α MAPK siRNA affected SDF-1β protection from palmitate-induced myocardial fibrosis measured by the expression of KLF15 and CTGF (Fig. 3A-B).

3.2 Conditional knockout of cardiac specific Klf15 gene aggravated the cardiac dysfunction and weakened protection of SDF-1β in T2D mice

Echocardiography (Table 1) revealed that T2D induced cardiac dysfunction and *Klf15*-cKO could also lead to cardiac dysfunction. *Klf15*-cKO aggravated T2D-induced cardiac dysfunction. The cardiac dysfunction was confirmed by decreased EF and FS (Table 1). SDF-1β treatment significantly improved EF and FS of the WT group, and it also significantly improved EF in *Klf15*-cKO group (Table 1), thus demonstrating that the protective effect of SDF-1β on DCM was not always dependent on the KLF15 pathway.

3.3 Conditional knockout of cardiac specific Klf15 gene aggravated the cardiac fibrosis and abolished protection of SDF-1β in T2D mice

To validate the *in vitro* findings we examined effects of *in vivo* loss of KLF15 expression with or without T2D on cardiac fibrosis. To this end, *Klf15*-cKO and WT mice were fed with HFD for 3 months to induce insulin resistance, and then these mice were injected with a single dose of STZ at 100 mg/kg body weight to induce T2D mouse model. After the onset of hyperglycemia, all T2D and age-matched control mice were treated with or without SDF-1β at 5 mg/kg body-weight twice a week for 3 months. At the end of the treatment, although blood glucose levels, total cholesterol and triglyceride levels were significantly increased in the T2D group both in WT group and *Klf15*-cKO group, SDF-1β treatment did not modulate these levels in both control and T2D groups (Fig. 4A-C). However, T2D as well as SDF-1β treatment did not affect the heart weight/tibia length ratio (Fig. 4D). Fibrotic response was examined by Sirius-red staining of collagen (38) (Fig. 4E). T2D was associated with a significant increase in cardiac fibrosis and *Klf15*-cKO significantly aggravated the damage of diabetes to myocardium, as shown by Sirius-red staining of collagen deposition (Fig. 4E). SDF-1β treatment significantly, but incompletely prevented the diabetes-induced cardiac fibrosis in WT group. However, in *Klf15*-cKO group, cardiac fibrosis was not alleviated by SDF-1β treatment (Fig. 4E). These results suggest that T2D-induced down-regulation of KLF15 was critical to cardiac fibrosis and the protective effect of SDF-1β on cardiac fibrosis was mediated by upregulating KLF15 expression in the heart, thus making KLF15 a key regulator of the cardioprotective effect of SDF-1β.

Next, the expressions of KLF15 and CTGF in the cardiac tissues of the *Klf15*-cKO and WT mice were measured by Western blotting. In WT group, T2D significantly decreased KLF15 protein level and significantly increased CTGF protein level (Fig. 5A), and SDF-1β significantly prevented the down-regulation of KLF15 expression and up-regulation of CTGF caused by T2D (Fig. 5A). *Klf15*-cKO significantly increased CTGF expression compared to the WT group, while the expression of CTGF was not different among groups with and without SDF-1β in *Klf15*-cKO/T2D mice group (Fig. 5A).

In both WT group and *Klf15*-cKO groups, T2D significantly increased collagen I, fibronectin and TGF-β1 protein levels in the cardiac tissues, and in WT group, SDF-1β significantly inhibited T2D-induced collagen I, fibronectin and TGF-β1 up-regulation. In *Klf15*-cKO/T2D mice, a more significant increase in collagen I, fibronectin and TGF-β1 protein levels were detected as compared to *Klf15*-cKO group, and the expression of collagen I, fibronectin and TGF-β1 were unaffected by SDF-1β treatment in *Klf15*-cKO/T2D mice (Fig. 5B).

3.4 Protective effect of SDF-1β on T2D-induced cardiac fibrosis is mediated by p38β MAPK up-regulation

Furthermore, because p38 MAPK plays an important role in protecting the heart under various conditions (30, 39–41) and we also demonstrated that p38β MAPK activation was required for SDF-1β's cardiac protection from palmitate-induced cardiac cell death (21), the level of *p*-p38 MAPK, p38 MAPK, p38α MAPK and p38β MAPK protein in the cardiac tissues were measured, and we found that SDF-1β induced

significant up-regulation of *p*-p38MAPK and p38β MAPK, but not p38α MAPK in T2D/SDF-1β and *Klf15*-cKO/T2D/SDF-1β groups compared to T2D and *Klf15*-cKO/T2D groups respectively (Fig. 6).

4. Discussion

Cardiac fibrosis is a hallmark feature of pathologic remodeling of the heart in response to hemodynamic or neurohormonal stress. In DCM, the pathogenesis is multifactorial and myocardial fibrosis is the frequently proposed mechanism to explain cardiac changes (42). The anti-fibrosis action of KLF15 is an important part of the cardioprotective mechanisms (24, 26, 27). Previous studies have shown that SDF-1 has a protective effect on the survival of hypoxic cardiomyocytes after myocardial infarction and ischemia/reperfusion injury (18–20, 43). In the current study we demonstrated that SDF-1β significantly inhibited myocardial fibrosis and significantly prevented the down-regulation of myocardial KLF15 expression caused by T2D (Fig. 5). Our findings shed new light on the mechanisms by which SDF-1β attenuates cardiac fibrosis through KLF15 dependent pathway in T2D mice. Here, we presented evidences that support the regulatory effect of KLF15 by SDF-1β in T2D mice.

KLF15 is highly expressed in the mouse heart tissue (44). Fisch *et.al* have identified KLF15 as a novel inhibitor of the heart's response to pressure overload through inhibition of the MEF2 and GATA4 transcriptional pathway (27). Wang *et.al* found that adenoviral overexpression of KLF15 also significantly inhibited the basal expression of CTGF of neonatal rat ventricular fibroblasts and the expression of CTGF induced by TGF-β1. After ligating the aorta of *Klf15* knockout mice, the expression of CTGF in the heart increased and the degree of cardiac fibrosis increased (26). The above studies have fully demonstrated that KLF15 is a key factor that negatively regulates myocardial fibrotic signaling pathway. In our study, we demonstrated that EF significantly declined (Table 1), with significant decrease in KLF15 expression and concurrent increase in CTGF expression in T2D group compared to WT group (Fig. 5). Moreover, in *Klf15*-cKO mice, EF significantly declined and the expression of CTGF significantly increased in the *Klf15*-cKO/T2D group compared with the *Klf15*-cKO group, confirming that KLF15 is a key negative regulator in modulating cardiac dysfunction and myocardial fibrosis induced by T2D (Table 1 and Fig. 5). After co-treatment with SDF-1β, EF significantly improved, and the expression of KLF15 in the heart of T2D mice was significantly increased (Table 1 and Fig. 5). We also demonstrated that the protective effect of SDF-1β on myocardial fibrosis in *Klf15*-cKO/T2D mice disappeared, proving that SDF-1β exerts anti-fibrosis effects through KLF15. However, in *Klf15*-cKO group, SDF-1β still significantly improved EF (Table 1). Previous studies have proved that in addition to myocardial fibrosis, there are a variety of molecular mechanisms that act synergistically to impair cardiac function and promote cardiomyocyte injury in diabetes, such as metabolic disturbances (45), small vessel disease (46), cardiac autonomic neuropathy (47), and insulin resistance (48), thus the protective effect of SDF-1β on DCM may not have merely been through inhibiting myocardial fibrosis.

SDF-1 regulates many essential biological processes, which has been considered predominantly through binding chemokine receptor, CXCR4 (7, 14). However, recent studies from us and others have implicated that SDF-1 can also bind chemokine receptor CXCR7 and can illicit different functions compared with

CXCR4, while playing an important role in mediating cell survival or the anti-apoptotic effect of SDF-1 (14, 21). Ding *et al* have confirmed the different effects of CXCR4 and CXCR7 on chronic liver injury, and found that during chronic liver injury, selective CXCR7 activation in liver sinusoidal endothelial cells promoted anti-fibrotic signaling, while loss of CXCR7 expression and the upregulation of CXCR4 expression promoted liver fibrosis (49). In our previous study, we have demonstrated that both CXCR4 and CXCR7 are expressed in cardiac H9C2 cells (21). *In vitro* studies, we also demonstrated that CXCR7 siRNA transfection completely blocked the myocardial protection of SDF-1β in palmitate treated H9C2 cells (Fig. 2A). However, CXCR4 siRNA transfection had no effect on the protective effect of SDF-1β on fibrosis of H9C2 cells (Fig. 3A). These findings suggested that the protective effect of SDF-1β on palmitate-induced cardiomyocyte fibrosis was mediated *via* binding to CXCR7 receptor.

Studies have shown that CXCR7 can activate MAPK signaling pathways (50). The MAPK signaling pathway allows cells to process a wide range of external signals and respond appropriately, generating a plethora of different biological effects. The diversity and specificity of cellular outcomes is achieved by functionally distinct p38 MAPK isoforms (51). The cardioprotective effect of p38β MAPK has been confirmed in different animal models. Venkatakrishnan *et al.* have shown that activation of the p38β MAPK attenuated doxorubicin-induced cardiotoxicity (52). In our previous study, we have also demonstrated that p38β MAPK activation was required for SDF-1β's cardiac protection from palmitate-induced cardiac cell death (21). In this study, we demonstrated that silencing p38β MAPK expression prevented upregulation of KLF15 expression in the presence of palmitate and SDF-1β, suggesting the direct requirement of p38β MAPK for the cardiac protection by SDF-1β (Fig. 2B).

5. Conclusions

In summary, the current study utilized *Klf15*-cKO mice for the first time and demonstrated that in T2D mice, SDF-1β attenuates cardiac fibrosis through KLF15 dependent pathway. The cardiac protective effect of SDF-1β was mediated by binding to CXCR7 receptor and by p38β MAPK-mediated KLF15 up-regulation. These findings demonstrate that KLF15 is a key negative regulator in the process of T2D-induced myocardial fibrosis, which may find serving as a new molecular target for the prevention and/or treatment of T2D-induced myocardial fibrosis, and may lead to the development of new drugs that promote KLF15 expression and treat DCM. Furthermore, these findings also provide a novel insight into the mechanism by which SDF-1β induced cardiac protection in T2D and SDF-1β may serve as a therapy in the prevention and treatment of DCM.

Abbreviations

DCM diabetic cardiomyopathy

HFD high fat diet

ND normal diet

DM diabetes mellitus

T2D type 2 diabetes

CVD cardiovascular disease

SDF-1 stromal cell-derived factor

KLFs krüppel-like factors

CTGF connective tissue growth factor

TGF-β tissue growth factor-β

LVH left ventricular hypertrophy

MEF2 myocyte enhancer factor 2

GATA4 GATA binding protein 4

LV left ventricular

p38 MAPK p38 mitogen activated protein kinase

EF ejection fraction

FS fractional shortening

BSA bovine serum albumin

PBS phosphate buffered saline

rAV recombinant adenovirus

MOI multiplicity of infection

Declarations

Ethics approval and consent to participate

All animal protocols were approved by the Animal Ethics Committee of Jilin University.

Consent for publication

Not applicable.

Availability of data and materials

All data generated or analysed during this study are included in this published article.

Competing interests

The authors declare that they have no competing interests.

Funding

This study was supported by grants from the National Science Foundation of China (81670221, 81974227 to YGZ).

Authors' contributions

YYT, ZYW, YGZ analyzed data, and wrote the manuscript. LC and MR interpreted experimental data and prepared and reviewed the manuscript. XYZ, SHC, WJS, ZJ discussed project progression, researched data, and reviewed the manuscript. YGZ contributed to the initial formulation of the project, discussed project progression, and wrote, reviewed, and edited the manuscript. YGZ is the guarantor of this work, and, as such, had full access to all the data in the study and takes full responsibility for the integrity of data and the accuracy of data analysis.

Acknowledgements

Not applicable.

References

1. Zheng Y, Ley SH, Hu FB. Global aetiology and epidemiology of type 2 diabetes mellitus and its complications. Nat Rev Endocrinol. 2018;14(2):88-98.
2. International Diabetes Federation. IDF Diabetes Atlas — 7th Edition. DiabetesAtlas. 2019. http://www.diabetesatlas.org/dose/international diabetes federation. Accessed Sept 2019.
3. Almourani R, Chinnakotla B, Patel R, Kurukulasuriya LR, Sowers J. Diabetes and Cardiovascular Disease: an Update. Curr Diab Rep. 2019;19(12):161.
4. Rubler S, Dlugash J, Yuceoglu YZ, Kumral T, Branwood AW, Grishman A. New type of cardiomyopathy associated with diabetic glomerulosclerosis. The American journal of cardiology. 1972;30(6):595-602.
5. Gray S, Kim JK. New insights into insulin resistance in the diabetic heart. Trends in endocrinology and metabolism: TEM. 2011;22(10):394-403.
6. Gerrits H, van Ingen Schenau DS, Bakker NE, van Disseldorp AJ, Strik A, Hermens LS, et al. Early postnatal lethality and cardiovascular defects in CXCR7-deficient mice. Genesis (New York, NY : 2000). 2008;46(5):235-45.
7. Tan Y, Li Y, Xiao J, Shao H, Ding C, Arteel GE, et al. A novel CXCR4 antagonist derived from human SDF-1beta enhances angiogenesis in ischaemic mice. Cardiovascular research. 2009;82(3):513-21.

8. Yu L, Cecil J, Peng SB, Schrementi J, Kovacevic S, Paul D, et al. Identification and expression of novel isoforms of human stromal cell-derived factor 1. Gene. 2006;374:174-9.
9. Altenburg JD, Broxmeyer HE, Jin Q, Cooper S, Basu S, Alkhatib G. A naturally occurring splice variant of CXCL12/stromal cell-derived factor 1 is a potent human immunodeficiency virus type 1 inhibitor with weak chemotaxis and cell survival activities. Journal of virology. 2007;81(15):8140-8.
10. Shirozu M, Nakano T, Inazawa J, Tashiro K, Tada H, Shinohara T, et al. Structure and chromosomal localization of the human stromal cell-derived factor 1 (SDF1) gene. Genomics. 1995;28(3):495-500.
11. Tashiro K, Tada H, Heilker R, Shirozu M, Nakano T, Honjo T. Signal sequence trap: a cloning strategy for secreted proteins and type I membrane proteins. Science (New York, NY). 1993;261(5121):600-3.
12. De La Luz Sierra M, Yang F, Narazaki M, Salvucci O, Davis D, Yarchoan R, et al. Differential processing of stromal-derived factor-1alpha and stromal-derived factor-1beta explains functional diversity. Blood. 2004;103(7):2452-9.
13. Janowski M. Functional diversity of SDF-1 splicing variants. Cell adhesion & migration. 2009;3(3):243-9.
14. Dai X, Tan Y, Cai S, Xiong X, Wang L, Ye Q, et al. The role of CXCR7 on the adhesion, proliferation and angiogenesis of endothelial progenitor cells. Journal of cellular and molecular medicine. 2011;15(6):1299-309.
15. Balabanian K, Lagane B, Infantino S, Chow KY, Harriague J, Moepps B, et al. The chemokine SDF-1/CXCL12 binds to and signals through the orphan receptor RDC1 in T lymphocytes. J Biol Chem. 2005;280(42):35760-6.
16. Burns JM, Summers BC, Wang Y, Melikian A, Berahovich R, Miao Z, et al. A novel chemokine receptor for SDF-1 and I-TAC involved in cell survival, cell adhesion, and tumor development. The Journal of experimental medicine. 2006;203(9):2201-13.
17. Shimizu S, Brown M, Sengupta R, Penfold ME, Meucci O. CXCR7 protein expression in human adult brain and differentiated neurons. Plos One. 2011;6(5):e20680.
18. Hu X, Dai S, Wu WJ, Tan W, Zhu X, Mu J, et al. Stromal cell derived factor-1 alpha confers protection against myocardial ischemia/reperfusion injury: role of the cardiac stromal cell derived factor-1 alpha CXCR4 axis. Circulation. 2007;116(6):654-63.
19. Segers VF, Tokunou T, Higgins LJ, MacGillivray C, Gannon J, Lee RT. Local delivery of protease-resistant stromal cell derived factor-1 for stem cell recruitment after myocardial infarction. Circulation. 2007;116(15):1683-92.
20. Saxena A, Fish JE, White MD, Yu S, Smyth JW, Shaw RM, et al. Stromal cell-derived factor-1alpha is cardioprotective after myocardial infarction. Circulation. 2008;117(17):2224-31.
21. Zhao Y, Tan Y, Xi S, Li Y, Li C, Cui J, et al. A novel mechanism by which SDF-1β protects cardiac cells from palmitate-induced endoplasmic reticulum stress and apoptosis via CXCR7 and AMPK/p38 MAPK-mediated interleukin-6 generation. Diabetes. 2013;62(7):2545-58.
22. Feinberg MW, Lin Z, Fisch S, Jain MK. An emerging role for Krüppel-like factors in vascular biology. Trends in cardiovascular medicine. 2004;14(6):241-6.

23. Bieker JJ. Krüppel-like factors: three fingers in many pies. J Biol Chem. 2001;276(37):34355-8.
24. Uchida S, Tanaka Y, Ito H, Saitoh-Ohara F, Inazawa J, Yokoyama KK, et al. Transcriptional regulation of the CLC-K1 promoter by myc-associated zinc finger protein and kidney-enriched Krüppel-like factor, a novel zinc finger repressor. Molecular and cellular biology. 2000;20(19):7319-31.
25. Yu Y, Ma J, Xiao Y, Yang Q, Kang H, Zhen J, et al. KLF15 is an essential negative regulatory factor for the cardiac remodeling response to pressure overload. Cardiology. 2015;130(3):143-52.
26. Wang B, Haldar SM, Lu Y, Ibrahim OA, Fisch S, Gray S, et al. The Kruppel-like factor KLF15 inhibits connective tissue growth factor (CTGF) expression in cardiac fibroblasts. Journal of molecular and cellular cardiology. 2008;45(2):193-7.
27. Fisch S, Gray S, Heymans S, Haldar SM, Wang B, Pfister O, et al. Kruppel-like factor 15 is a regulator of cardiomyocyte hypertrophy. Proceedings of the National Academy of Sciences of the United States of America. 2007;104(17):7074-9.
28. Patel SK, Wai B, Lang CC, Levin D, Palmer CNA, Parry HM, et al. Genetic Variation in Kruppel like Factor 15 Is Associated with Left Ventricular Hypertrophy in Patients with Type 2 Diabetes: Discovery and Replication Cohorts. EBioMedicine. 2017;18:171-8.
29. Zhao Y, Cai L. Does Krüppel Like Factor 15 Play an Important Role in the Left Ventricular Hypertrophy of Patients with Type 2 Diabetes? EBioMedicine. 2017;20:17-8.
30. Leenders JJ, Wijnen WJ, Hiller M, van der Made I, Lentink V, van Leeuwen RE, et al. Regulation of cardiac gene expression by KLF15, a repressor of myocardin activity. J Biol Chem. 2010;285(35):27449-56.
31. Cuenda A, Rousseau S. p38 MAP-kinases pathway regulation, function and role in human diseases. Biochimica et biophysica acta. 2007;1773(8):1358-75.
32. Jiang Y, Gram H, Zhao M, New L, Gu J, Feng L, et al. Characterization of the structure and function of the fourth member of p38 group mitogen-activated protein kinases, p38delta. J Biol Chem. 1997;272(48):30122-8.
33. Dai X, Tan Y, Cai S, Xiong X, Wang L, Ye Q, et al. The role of CXCR7 on the adhesion, proliferation and angiogenesis of endothelial progenitor cells. J Cell Mol Med. 2011;15(6):1299-309.
34. Lu YY, Li XD, Zhou HD, Shao S, He S, Hong MN, et al. Transactivation domain of Krüppel-like factor 15 negatively regulates angiotensin II-induced adventitial inflammation and fibrosis. Faseb J. 2019;33(5):6254-68.
35. Luo G, Jian Z, Zhu Y, Zhu Y, Chen B, Ma R, et al. Sirt1 promotes autophagy and inhibits apoptosis to protect cardiomyocytes from hypoxic stress. Int J Mol Med. 2019;43(5):2033-43.
36. Bai Y, Cui W, Xin Y, Miao X, Barati MT, Zhang C, et al. Prevention by sulforaphane of diabetic cardiomyopathy is associated with up-regulation of Nrf2 expression and transcription activation. Journal of molecular and cellular cardiology. 2013;57:82-95.
37. Cai L, Chen S, Evans T, Deng DX, Mukherjee K, Chakrabarti S. Apoptotic germ-cell death and testicular damage in experimental diabetes: prevention by endothelin antagonism. Urological research. 2000;28(5):342-7.

38. Tan Y, Li X, Prabhu SD, Brittian KR, Chen Q, Yin X, et al. Angiotensin II plays a critical role in alcohol-induced cardiac nitrative damage, cell death, remodeling, and cardiomyopathy in a protein kinase C/nicotinamide adenine dinucleotide phosphate oxidase-dependent manner. Journal of the American College of Cardiology. 2012;59(16):1477-86.
39. Du JH, Xu N, Song Y, Xu M, Lu ZZ, Han C, et al. AICAR stimulates IL-6 production via p38 MAPK in cardiac fibroblasts in adult mice: a possible role for AMPK. Biochemical and biophysical research communications. 2005;337(4):1139-44.
40. Craig R, Larkin A, Mingo AM, Thuerauf DJ, Andrews C, McDonough PM, et al. p38 MAPK and NF-kappa B collaborate to induce interleukin-6 gene expression and release. Evidence for a cytoprotective autocrine signaling pathway in a cardiac myocyte model system. J Biol Chem. 2000;275(31):23814-24.
41. Tang CH, Chiu YC, Tan TW, Yang RS, Fu WM. Adiponectin enhances IL-6 production in human synovial fibroblast via an AdipoR1 receptor, AMPK, p38, and NF-kappa B pathway. Journal of immunology (Baltimore, Md : 1950). 2007;179(8):5483-92.
42. Fang ZY, Prins JB, Marwick TH. Diabetic cardiomyopathy: evidence, mechanisms, and therapeutic implications. Endocrine reviews. 2004;25(4):543-67.
43. Chen D, Xia Y, Zuo K, Wang Y, Zhang S, Kuang D, et al. Crosstalk between SDF-1/CXCR4 and SDF-1/CXCR7 in cardiac stem cell migration. Sci Rep. 2015;5:16813.
44. Gray S, Feinberg MW, Hull S, Kuo CT, Watanabe M, Sen-Banerjee S, et al. The Krüppel-like factor KLF15 regulates the insulin-sensitive glucose transporter GLUT4. J Biol Chem. 2002;277(37):34322-8.
45. Belke DD, Larsen TS, Gibbs EM, Severson DL. Altered metabolism causes cardiac dysfunction in perfused hearts from diabetic (db/db) mice. American journal of physiology Endocrinology and metabolism. 2000;279(5):E1104-13.
46. Hamby RI, Zoneraich S, Sherman L. Diabetic cardiomyopathy. Jama. 1974;229(13):1749-54.
47. Turpeinen AK, Vanninen E, Kuikka JT, Uusitupa MI. Demonstration of regional sympathetic denervation of the heart in diabetes. Comparison between patients with NIDDM and IDDM. Diabetes care. 1996;19(10):1083-90.
48. Hirayama H, Sugano M, Abe N, Yonemoch H, Makino N. Troglitazone, an antidiabetic drug, improves left ventricular mass and diastolic function in normotensive diabetic patients. Int J Cardiol. 2001;77(1):75-9.
49. Ding BS, Cao Z, Lis R, Nolan DJ, Guo P, Simons M, et al. Divergent angiocrine signals from vascular niche balance liver regeneration and fibrosis. Nature. 2014;505(7481):97-102.
50. Grymula K, Tarnowski M, Wysoczynski M, Drukala J, Barr FG, Ratajczak J, et al. Overlapping and distinct role of CXCR7-SDF-1/ITAC and CXCR4-SDF-1 axes in regulating metastatic behavior of human rhabdomyosarcomas. Int J Cancer. 2010;127(11):2554-68.
51. Cuadrado A, Nebreda AR. Mechanisms and functions of p38 MAPK signalling. The Biochemical journal. 2010;429(3):403-17.

52. Venkatakrishnan CD, Tewari AK, Moldovan L, Cardounel AJ, Zweier JL, Kuppusamy P, et al. Heat shock protects cardiac cells from doxorubicin-induced toxicity by activating p38 MAPK and phosphorylation of small heat shock protein 27. American journal of physiology Heart and circulatory physiology. 2006;291(6):H2680-91.

Figures

In vitro data

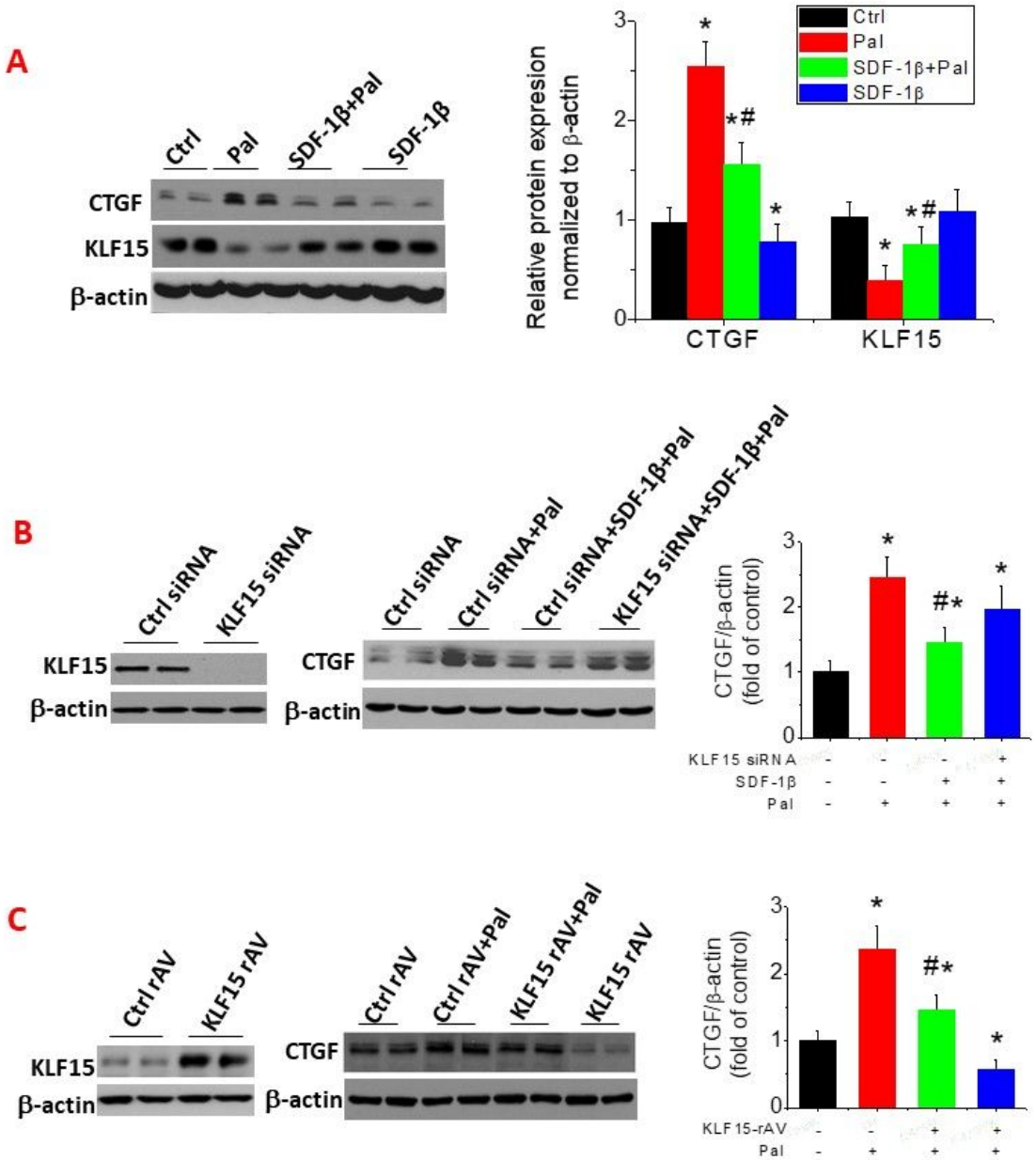

Fig. 1

Figure 1

Effects of SDF-1β on palmitate-induced myocardial fibrosis were mediated by up-regulating KLF15 in H9C2 cells. Embryonic rat heart derived H9C2 cells exposed to palmitate at 62.5 μM or vehicle were co-treated with or without 100 nM SDF-1 for 15 h. Myocardial fibrosis was examined by western blotting assay for CTGF expression (A, B, C). The KLF15 siRNA transfection was used to down-regulate KLF15 in H9C2 cells and the effects of down-regulating KLF15 expression in H9C2 cells on CTGF expression in presence of palmitate and SDF-1 was examined (B). The KLF15 recombinant adenovirus was used to up-regulate KLF15 in H9C2 cells and the effects of up-regulating KLF15 expression on CTGF expression in the presence and absence of palmitate was examined (C). The KLF15 expression was examined by western blotting assay (A, B, C). Data are presented as mean ± SD from at least three separate experiments. Ctrl, control; Pal, palmitate. *, $P<0.05$ vs control group; #, $P<0.05$ vs palmitate group.

In vitro data

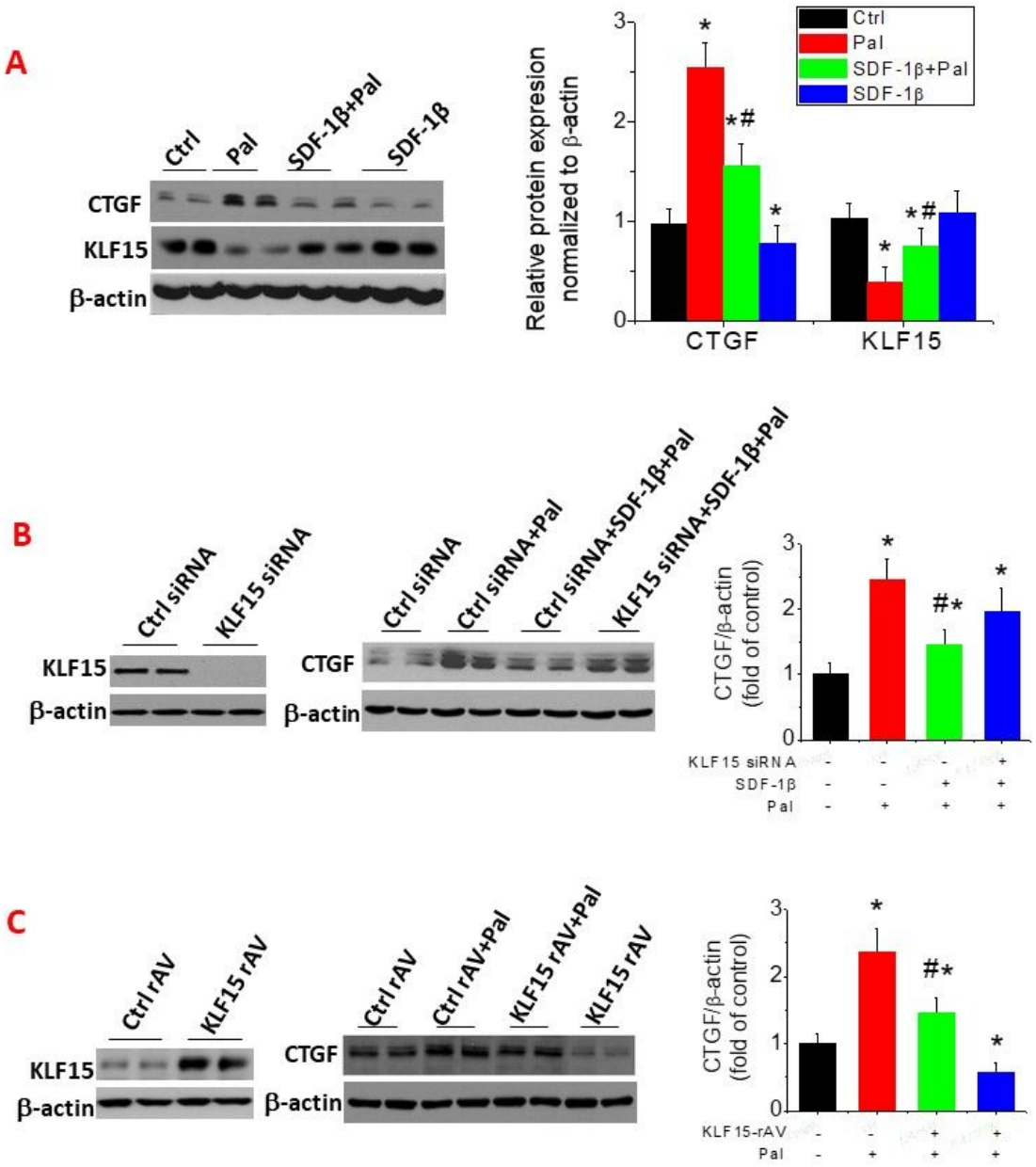

Fig. 1

Figure 1

Effects of SDF-1β on palmitate-induced myocardial fibrosis were mediated by up-regulating KLF15 in H9C2 cells. Embryonic rat heart derived H9C2 cells exposed to palmitate at 62.5 μM or vehicle were co-treated with or without 100 nM SDF-1 for 15 h. Myocardial fibrosis was examined by western blotting assay for CTGF expression (A, B, C). The KLF15 siRNA transfection was used to down-regulate KLF15 in H9C2 cells and the effects of down-regulating KLF15 expression in H9C2 cells on CTGF expression in

presence of palmitate and SDF-1β was examined (B). The KLF15 recombinant adenovirus was used to up-regulate KLF15 in H9C2 cells and the effects of up-regulating KLF15 expression on CTGF expression in the presence and absence of palmitate was examined (C). The KLF15 expression was examined by western blotting assay (A, B, C). Data are presented as mean ± SD from at least three separate experiments. Ctrl, control; Pal, palmitate. *, P<0.05 vs control group; #, P<0.05 vs palmitate group.

***In vitro* data**

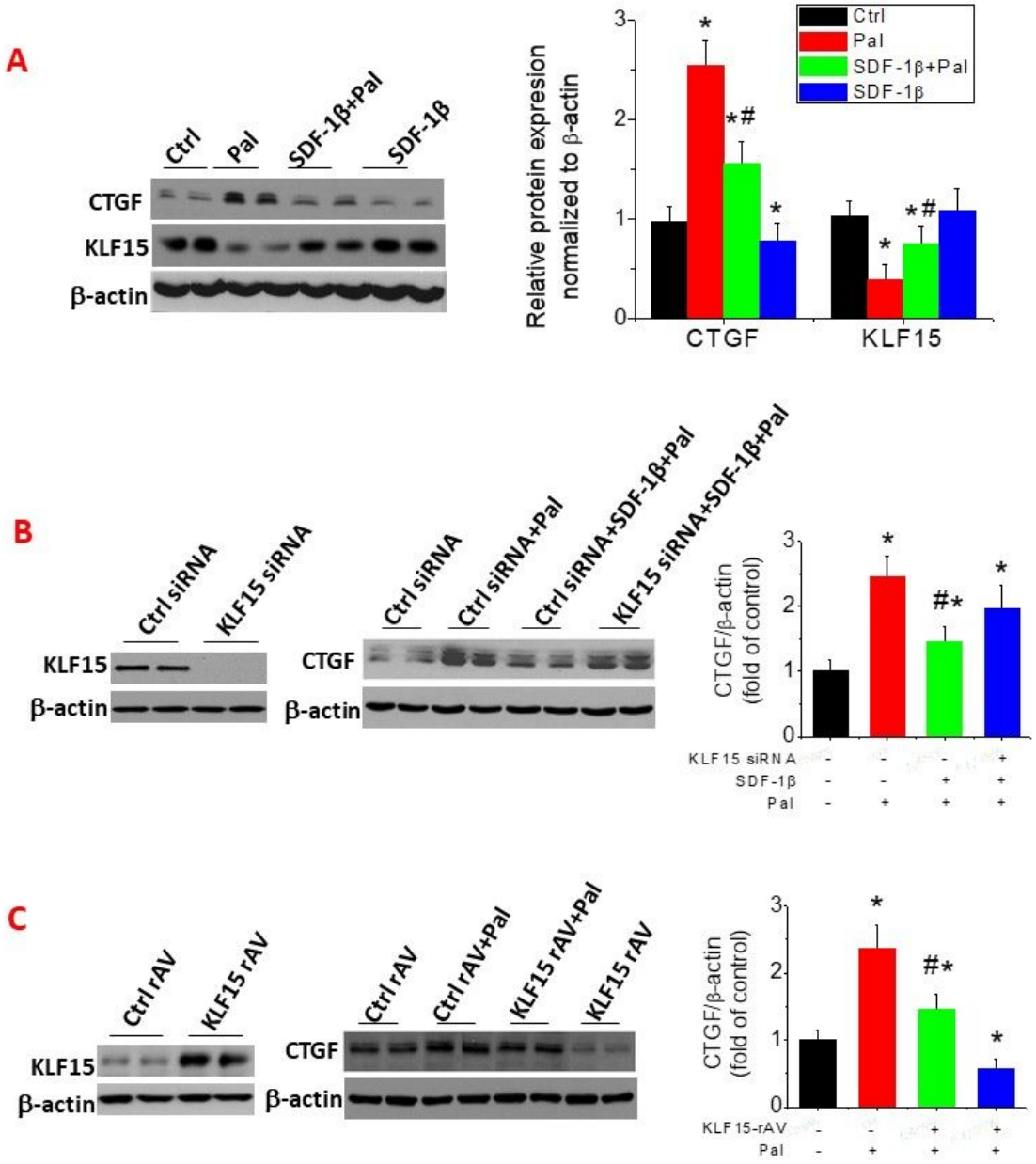

Fig. 1

Figure 1

Effects of SDF-1β on palmitate-induced myocardial fibrosis were mediated by up-regulating KLF15 in H9C2 cells. Embryonic rat heart derived H9C2 cells exposed to palmitate at 62.5 μM or vehicle were co-treated with or without 100 nM SDF-1 for 15 h. Myocardial fibrosis was examined by western blotting assay for CTGF expression (A, B, C). The KLF15 siRNA transfection was used to down-regulate KLF15 in H9C2 cells and the effects of down-regulating KLF15 expression in H9C2 cells on CTGF expression in presence of palmitate and SDF-1 was examined (B). The KLF15 recombinant adenovirus was used to up-regulate KLF15 in H9C2 cells and the effects of up-regulating KLF15 expression on CTGF expression in the presence and absence of palmitate was examined (C). The KLF15 expression was examined by western blotting assay (A, B, C). Data are presented as mean ± SD from at least three separate experiments. Ctrl, control; Pal, palmitate. *, $P<0.05$ vs control group; #, $P<0.05$ vs palmitate group.

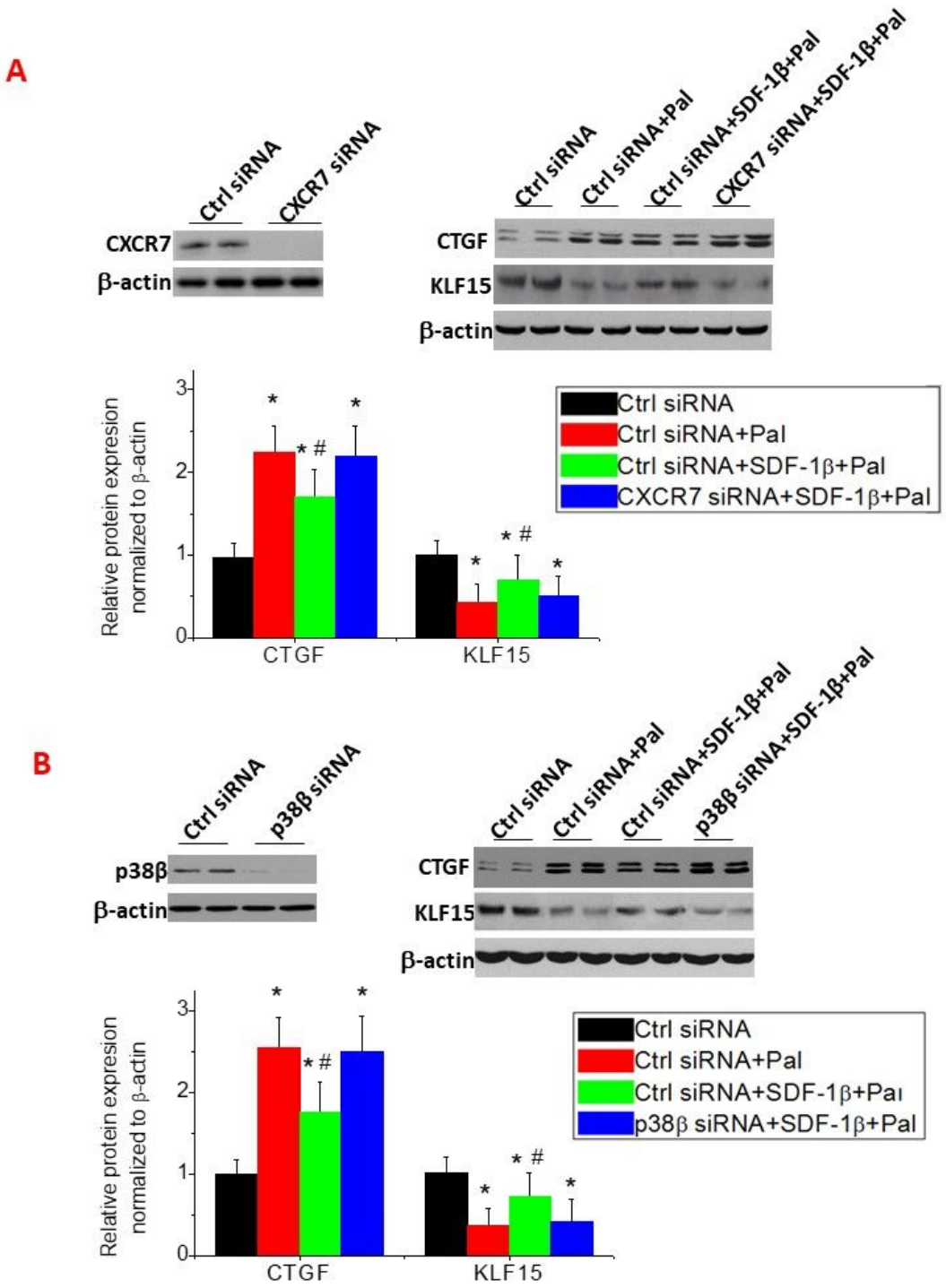

Fig. 2

Figure 2

SDF-1β inhibited palmitate-induced myocardial fibrosis via its receptor CXCR7 and p38β MAPK. H9C2 cells were subjected to the same treatment, as described in Fig. 1. The CXCR7 siRNA transfection was used to down-regulate CXCR7 in H9C2 cells and the effects of down-regulating CXCR7 expression in H9C2 cells on CTGF expression in presence of palmitate and SDF-1 was examined (A). The p38β MAPK siRNA transfection was used to down-regulate p38β MAPK in H9C2 cells and the effects of down-

regulating p38β expression in H9C2 cells on CTGF expression in the presence of palmitate and SDF-1β was examined (B). The expression of KLF15 and CTGF were measured by western blotting assay (A, B). Data are presented as mean ± SD from at least three separate experiments. Ctrl, control; Pal, palmitate.*, P<0.05 vs control group; #, P<0.05 vs palmitate group.

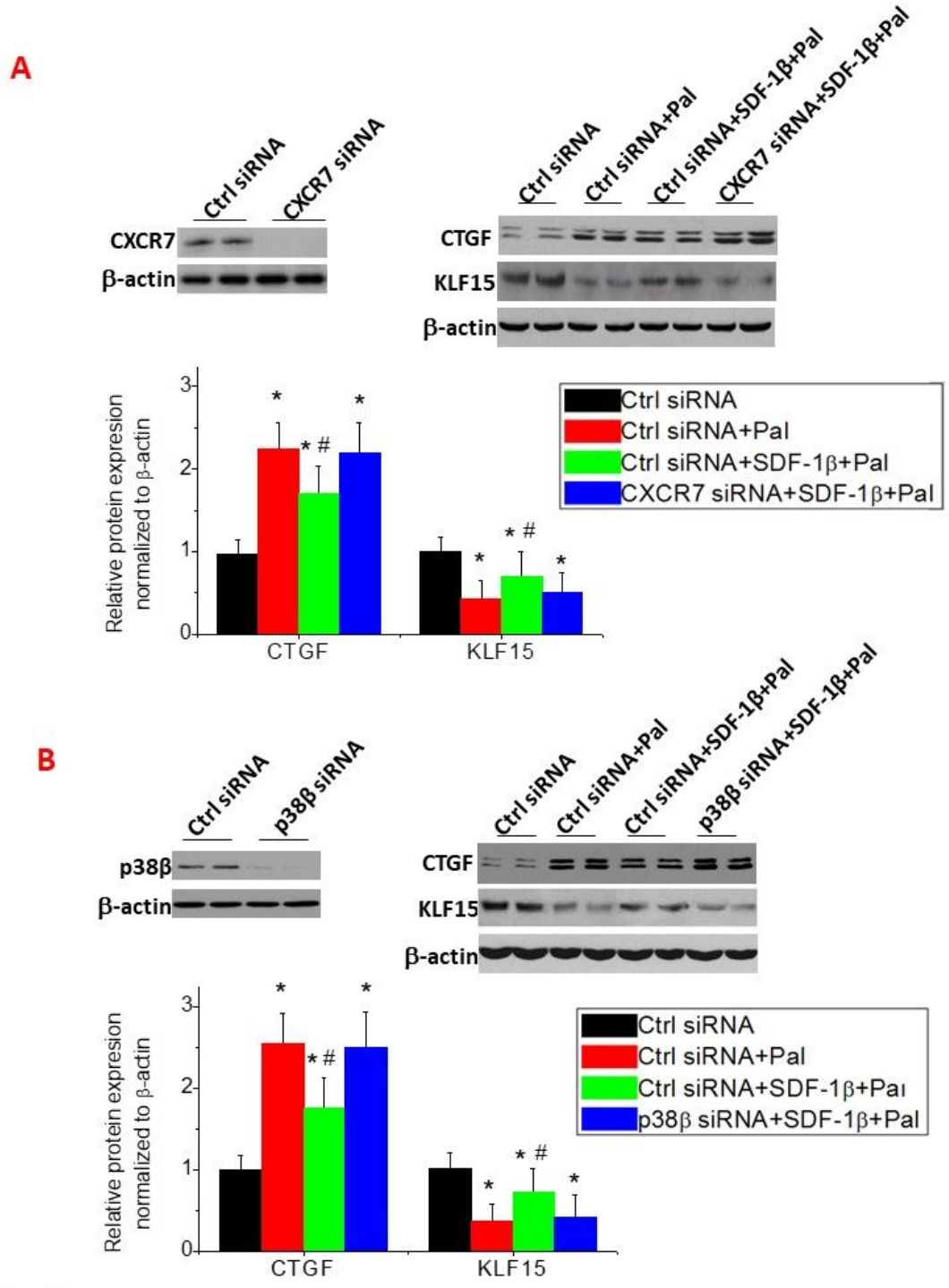

Fig. 2

Figure 2

SDF-1β inhibited palmitate-induced myocardial fibrosis via its receptor CXCR7 and p38β MAPK. H9C2 cells were subjected to the same treatment, as described in Fig. 1. The CXCR7 siRNA transfection was used to down-regulate CXCR7 in H9C2 cells and the effects of down-regulating CXCR7 expression in H9C2 cells on CTGF expression in presence of palmitate and SDF-1 was examined (A). The p38β MAPK siRNA transfection was used to down-regulate p38β MAPK in H9C2 cells and the effects of down-regulating p38 expression in H9C2 cells on CTGF expression in the presence of palmitate and SDF-1 was examined (B). The expression of KLF15 and CTGF were measured by western blotting assay (A, B). Data are presented as mean ± SD from at least three separate experiments. Ctrl, control; Pal, palmitate.*, P<0.05 vs control group; #, P<0.05 vs palmitate group.

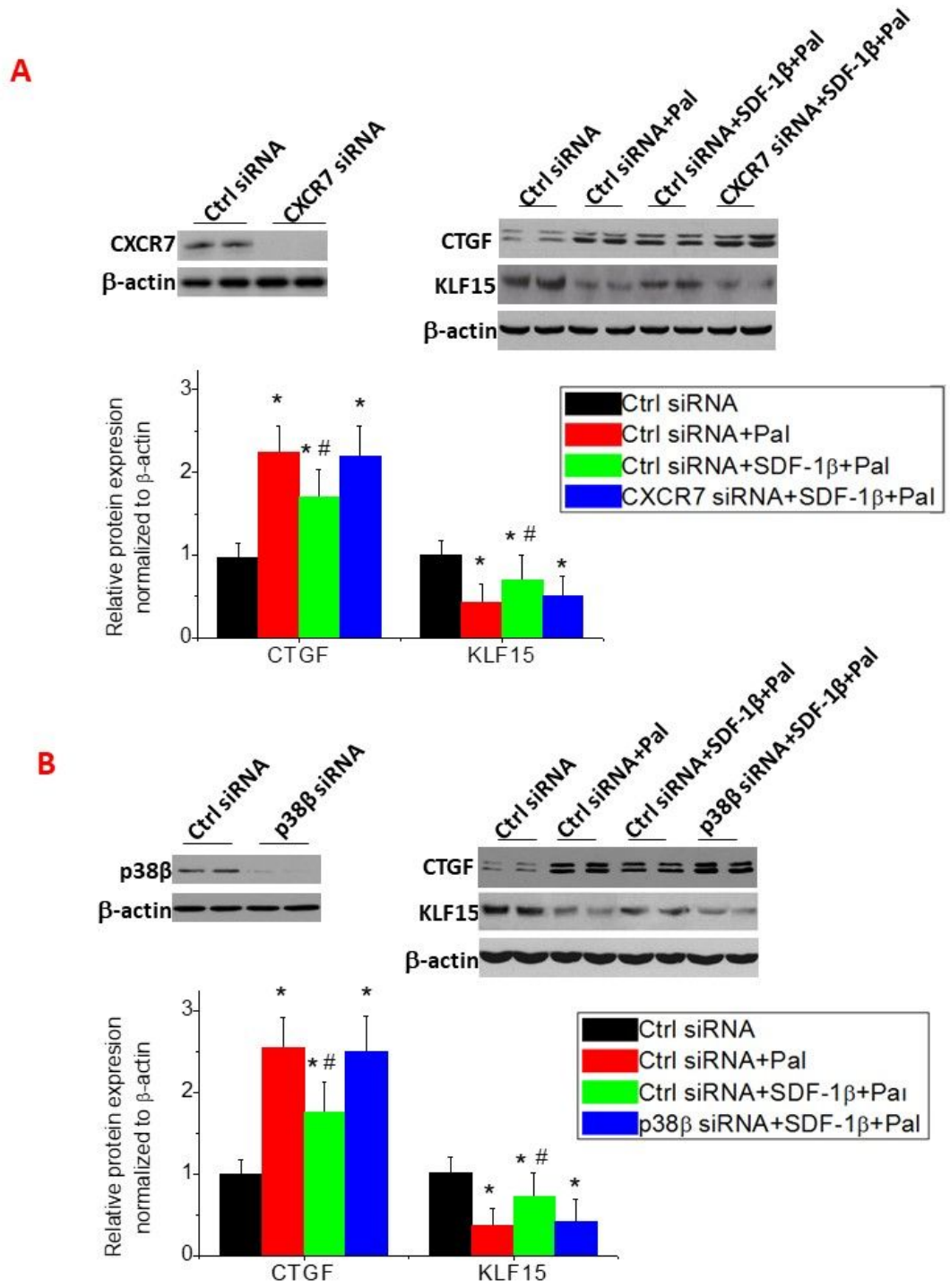

Fig. 2

Figure 2

SDF-1β inhibited palmitate-induced myocardial fibrosis via its receptor CXCR7 and p38β MAPK. H9C2 cells were subjected to the same treatment, as described in Fig. 1. The CXCR7 siRNA transfection was used to down-regulate CXCR7 in H9C2 cells and the effects of down-regulating CXCR7 expression in H9C2 cells on CTGF expression in presence of palmitate and SDF-1 was examined (A). The p38β MAPK siRNA transfection was used to down-regulate p38β MAPK in H9C2 cells and the effects of down-

regulating p38α expression in H9C2 cells on CTGF expression in the presence of palmitate and SDF-1β was examined (B). The expression of KLF15 and CTGF were measured by western blotting assay (A, B). Data are presented as mean ± SD from at least three separate experiments. Ctrl, control; Pal, palmitate.*, P<0.05 vs control group; #, P<0.05 vs palmitate group.

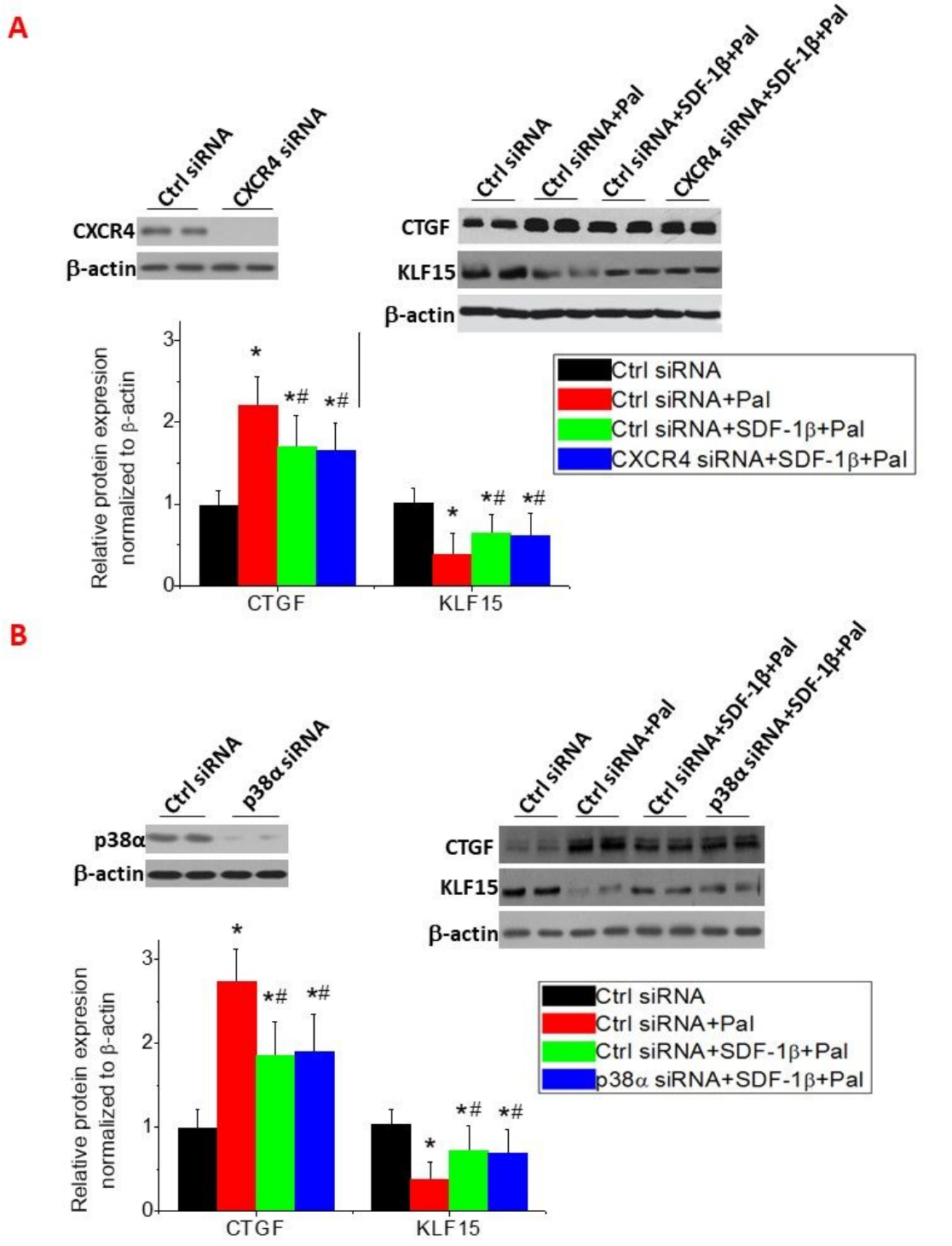

Fig. 3

Figure 3

Protective effect of SDF-1β on palmitate-induced myocardial fibrosis were not through CXCR4 and p38α MAPK. H9C2 cells were subjected to the same treatment, as described in Fig. 1. The CXCR4 siRNA transfection was used to down-regulate CXCR4 in H9C2 cells (A). The p38α MAPK siRNA transfection was used to down-regulate p38α MAPK in H9C2 cells (B). The expression of KLF15 and CTGF were measured by western blotting assay (A, B). Data are presented as mean ± SD from at least three separate experiments. Ctrl, control; Pal, palmitate.*, P<0.05 vs control group; #, P<0.05 vs palmitate group.

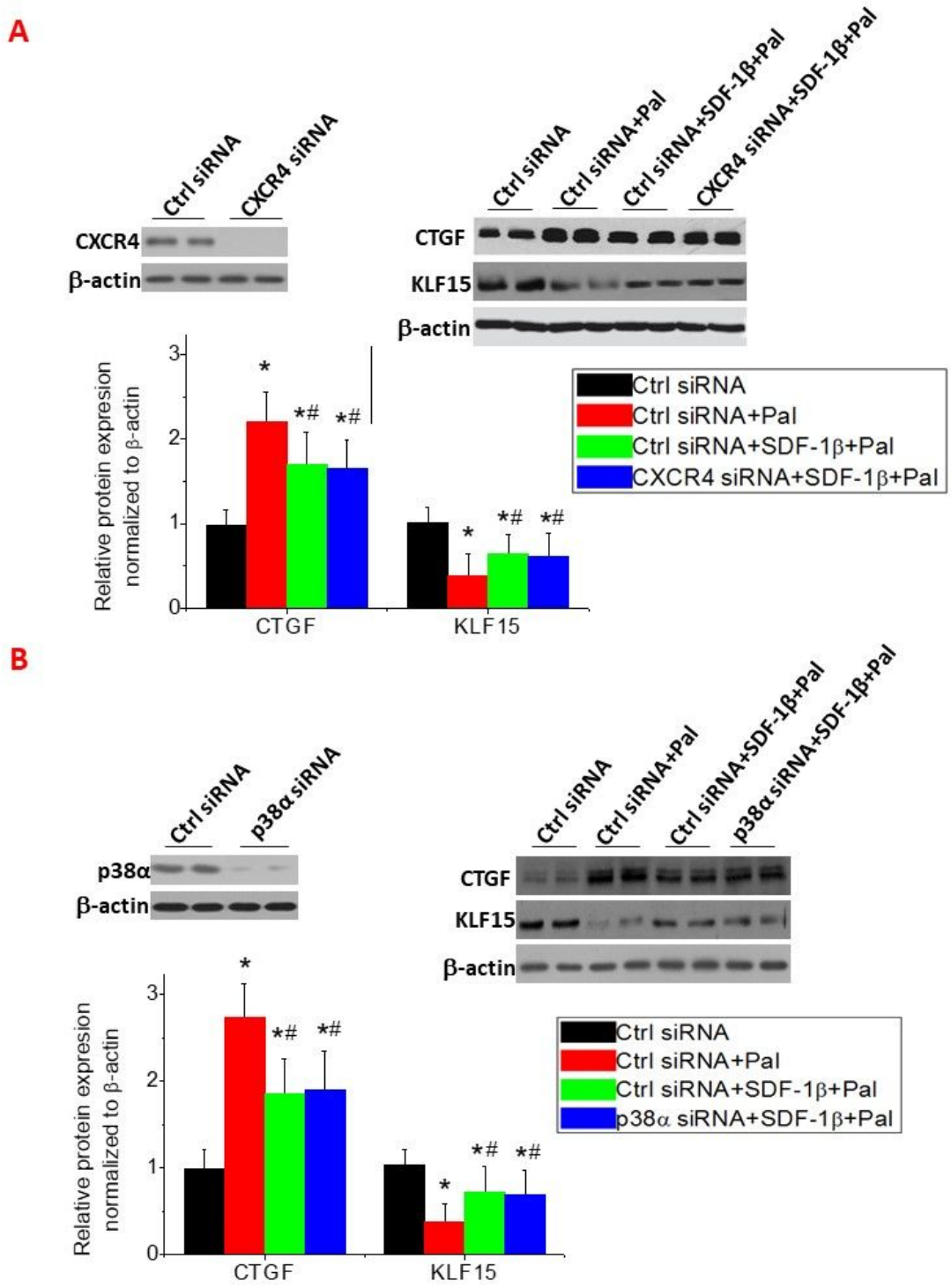

Fig. 3

Figure 3

Protective effect of SDF-1β on palmitate-induced myocardial fibrosis were not through CXCR4 and p38α MAPK. H9C2 cells were subjected to the same treatment, as described in Fig. 1. The CXCR4 siRNA transfection was used to down-regulate CXCR4 in H9C2 cells (A). The p38α MAPK siRNA transfection was used to down-regulate p38α MAPK in H9C2 cells (B). The expression of KLF15 and CTGF were measured by western blotting assay (A, B). Data are presented as mean ± SD from at least three separate experiments. Ctrl, control; Pal, palmitate.*, P<0.05 vs control group; #, P<0.05 vs palmitate group.

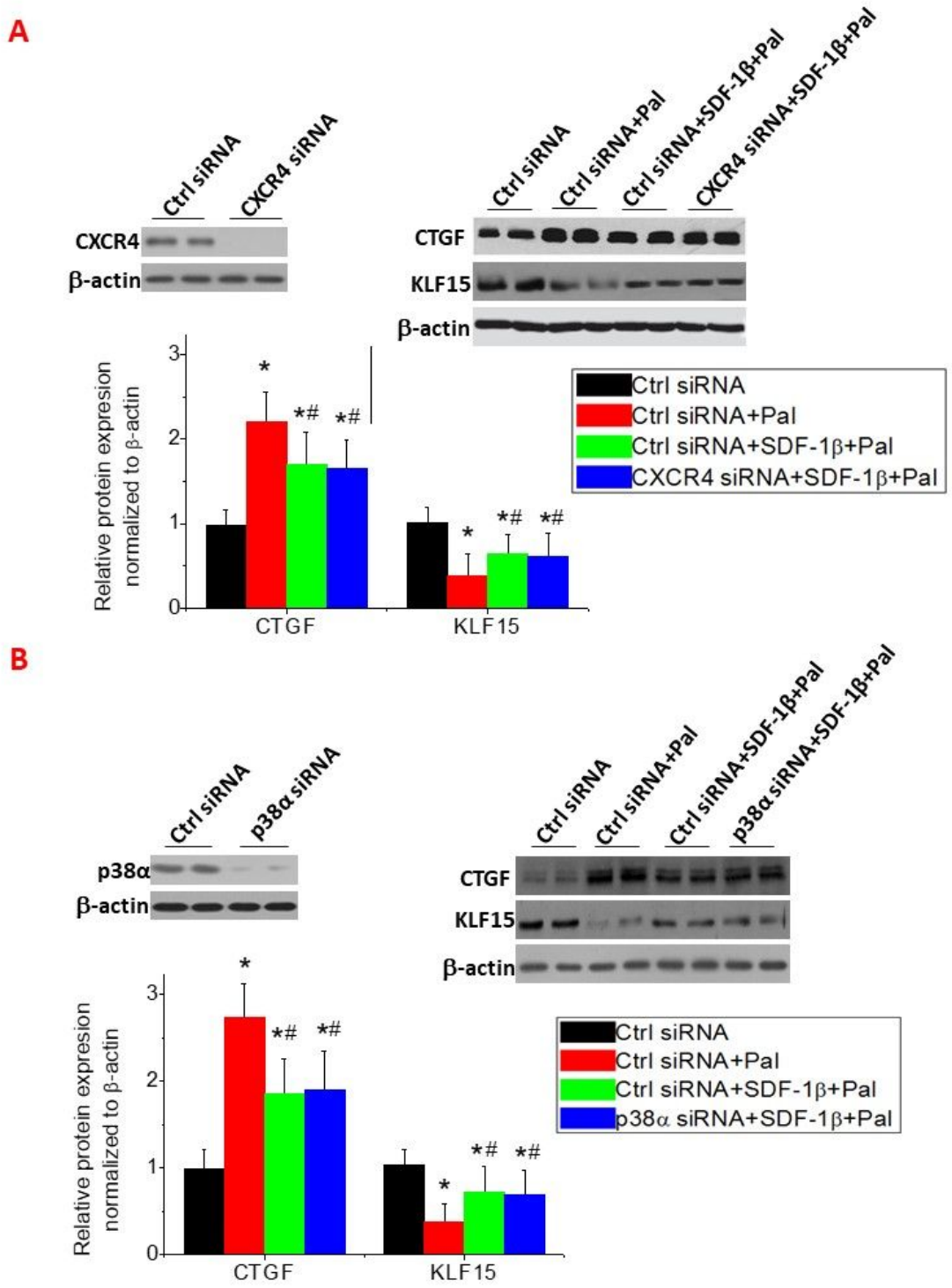

Fig. 3

Figure 3

Protective effect of SDF-1β on palmitate-induced myocardial fibrosis were not through CXCR4 and p38α MAPK. H9C2 cells were subjected to the same treatment, as described in Fig. 1. The CXCR4 siRNA transfection was used to down-regulate CXCR4 in H9C2 cells (A). The p38α MAPK siRNA transfection was used to down-regulate p38α MAPK in H9C2 cells (B). The expression of KLF15 and CTGF were measured by western blotting assay (A, B). Data are presented as mean ± SD from at least three separate experiments. Ctrl, control; Pal, palmitate.*, P<0.05 vs control group; #, P<0.05 vs palmitate group.

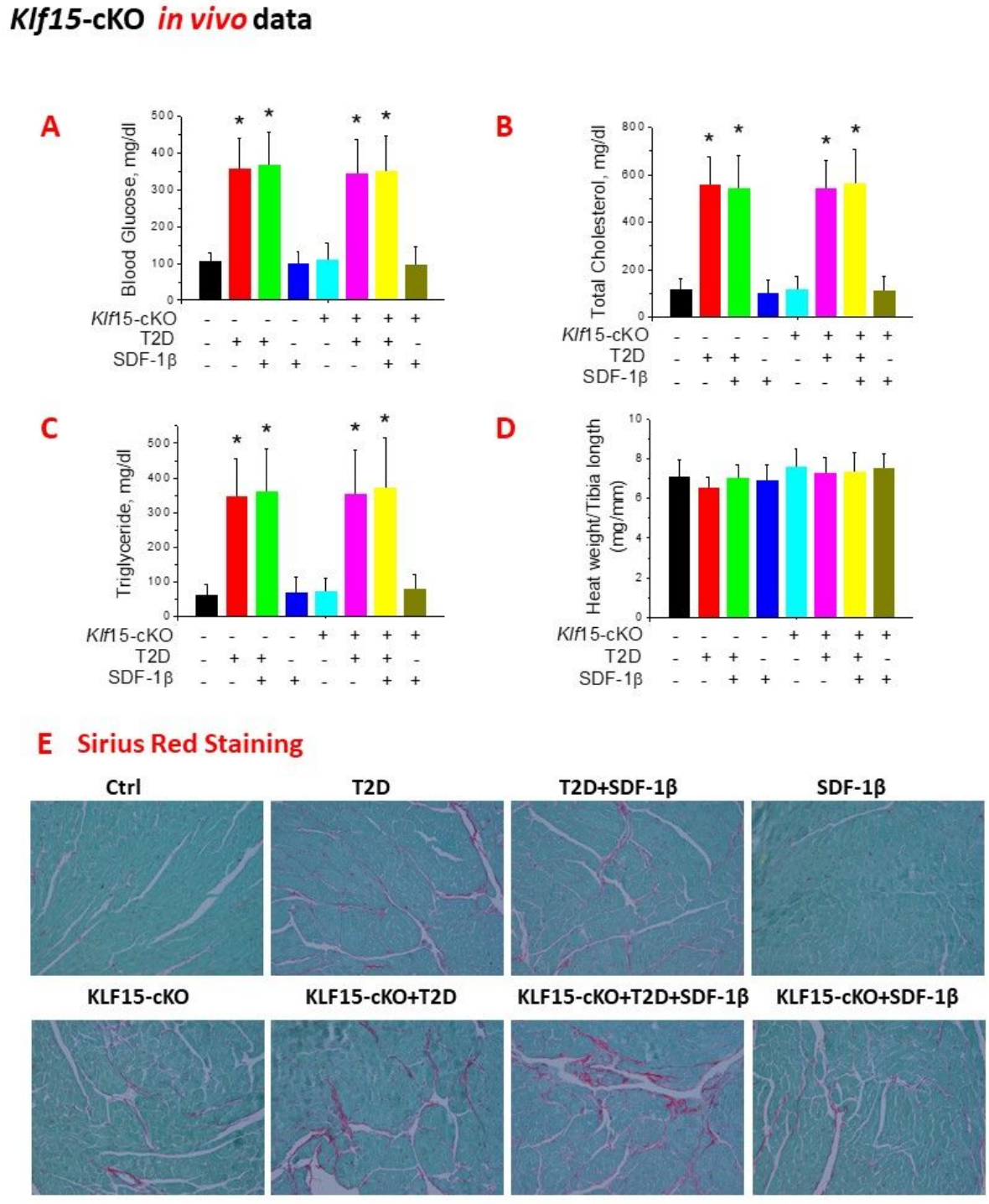

Fig. 4

Figure 4

Klf15-cKO aggravated the cardiac fibrosis and abolished protection of SDF-1β in T2D mice. Klf15-cKO and WT mice were fed with HFD for 3 months to induce insulin resistance, and then these mice were injected with a single dose of STZ at 100 mg/kg body weight to induce T2D model. After the onset of hyperglycemia, all T2D and age-matched control mice were treated with or without SDF-1β at 5 mg/kg body-weight twice a week for 3 months. At the end of the treatment, blood glucose (A), total cholesterol (B), triglyceride (C) and heart weight/tibia length ratio (D) were determined. Fibrotic response was examined by Sirius-red staining of collagen (E). Data are presented as mean ± SD (n = 6 at least in each group). Ctrl, control; T2D, type 2 diabetes; *, $P < 0.05$ vs. control group.

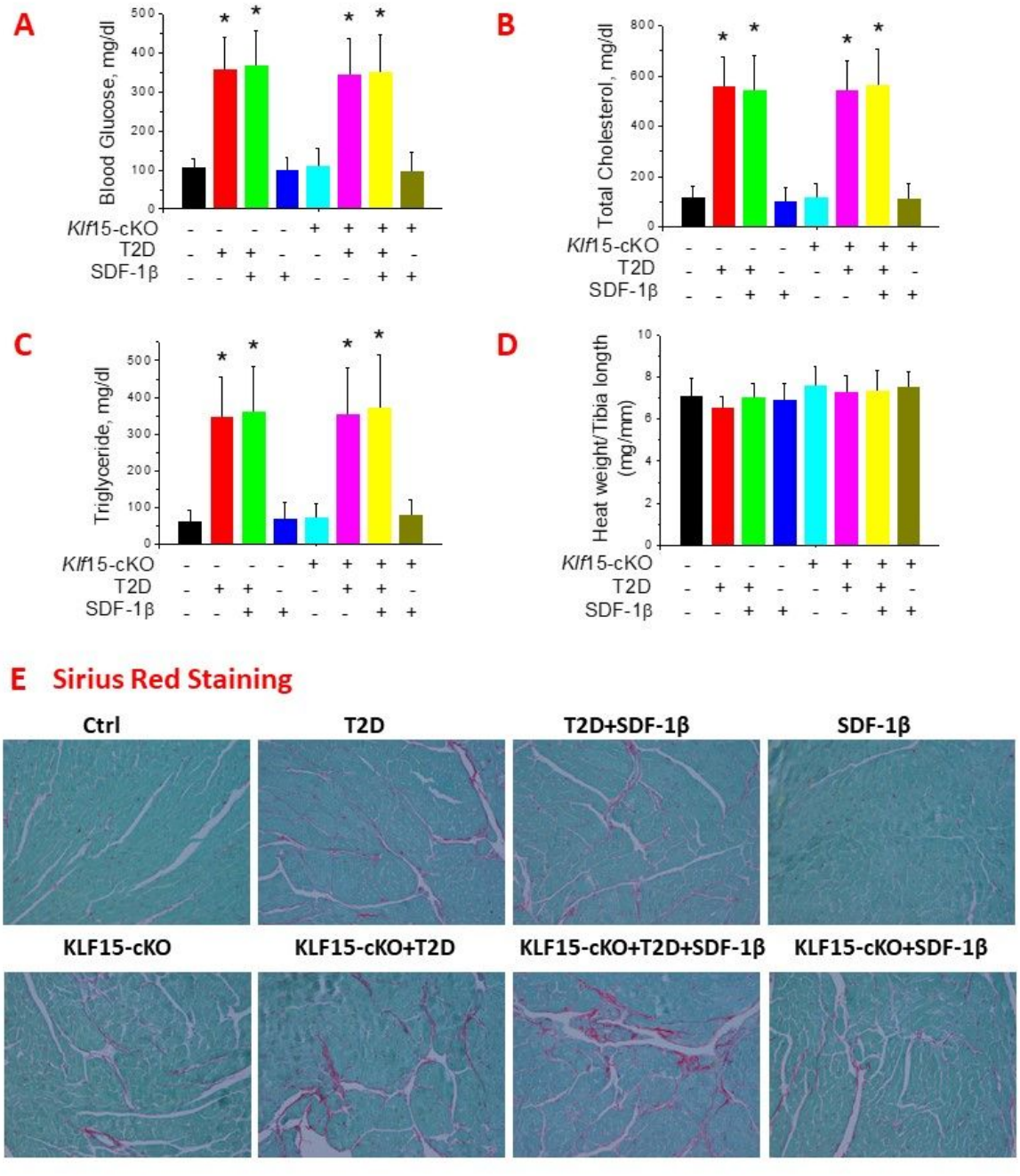

Fig. 4

Figure 4

Klf15-cKO aggravated the cardiac fibrosis and abolished protection of SDF-1β in T2D mice. Klf15-cKO and WT mice were fed with HFD for 3 months to induce insulin resistance, and then these mice were injected with a single dose of STZ at 100 mg/kg body weight to induce T2D model. After the onset of hyperglycemia, all T2D and age-matched control mice were treated with or without SDF-1β at 5 mg/kg body-weight twice a week for 3 months. At the end of the treatment, blood glucose (A), total cholesterol

(B), triglyceride (C) and heart weight/tibia length ratio (D) were determined. Fibrotic response was examined by Sirius-red staining of collagen (E). Data are presented as mean ± SD (n = 6 at least in each group). Ctrl, control; T2D, type 2 diabetes; *, P < 0.05 vs. control group.

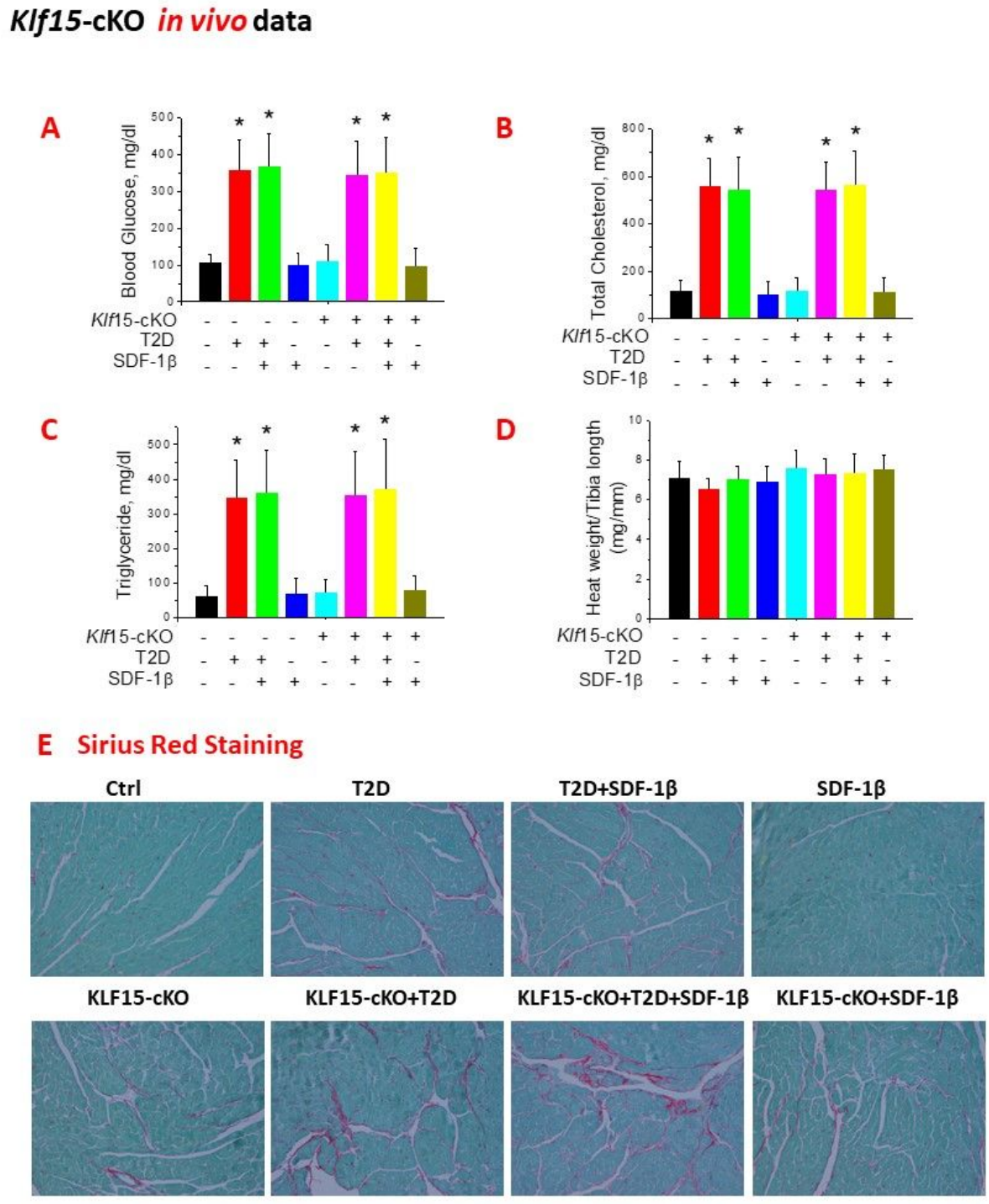

Fig. 4

Figure 4

Klf15-cKO aggravated the cardiac fibrosis and abolished protection of SDF-1β in T2D mice. Klf15-cKO and WT mice were fed with HFD for 3 months to induce insulin resistance, and then these mice were

injected with a single dose of STZ at 100 mg/kg body weight to induce T2D model. After the onset of hyperglycemia, all T2D and age-matched control mice were treated with or without SDF-1β at 5 mg/kg body-weight twice a week for 3 months. At the end of the treatment, blood glucose (A), total cholesterol (B), triglyceride (C) and heart weight/tibia length ratio (D) were determined. Fibrotic response was examined by Sirius-red staining of collagen (E). Data are presented as mean ± SD (n = 6 at least in each group). Ctrl, control; T2D, type 2 diabetes; *, P < 0.05 vs. control group.

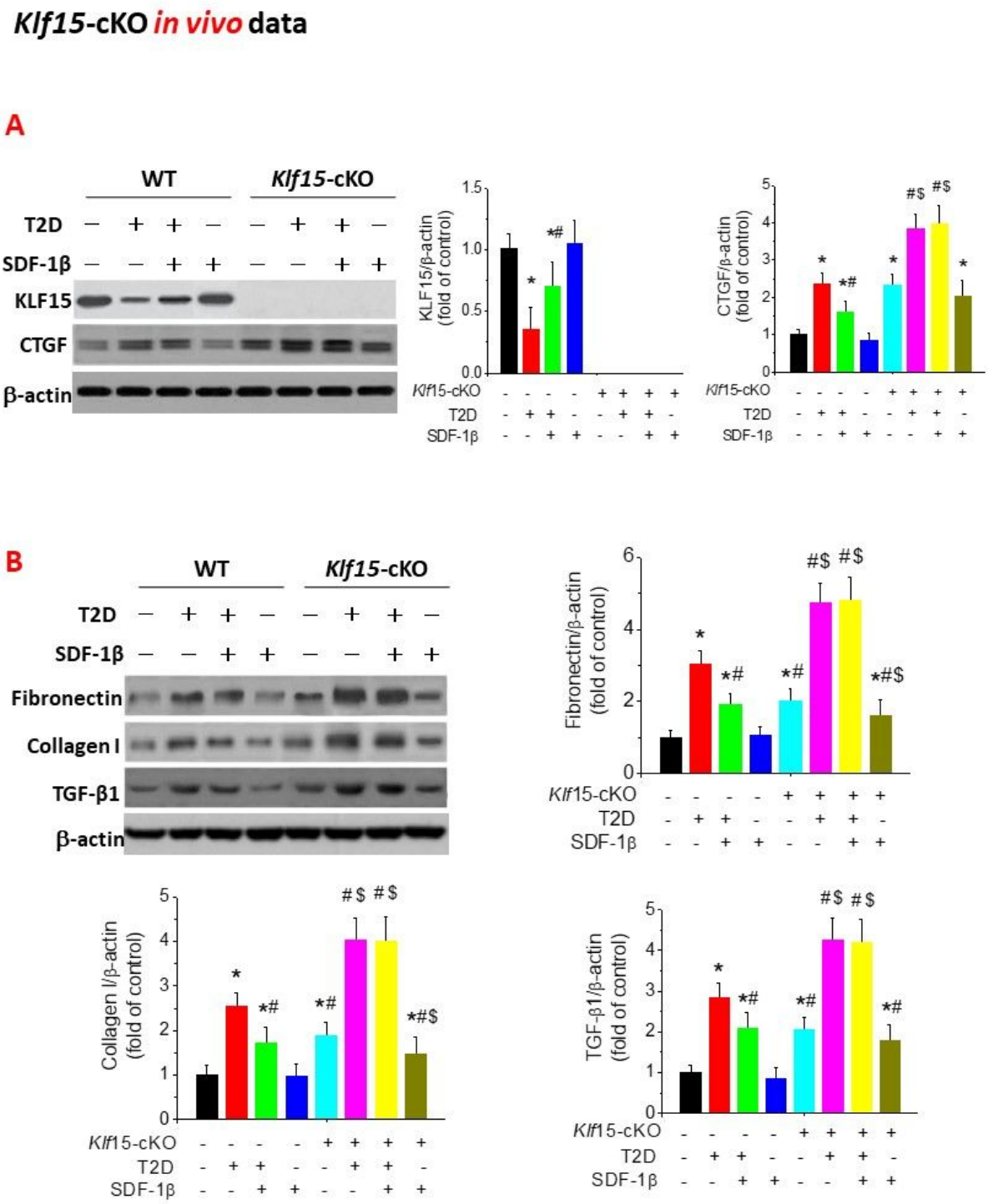

Fig. 5

Figure 5

Klf15-cKO aggravated the cardiac fibrosis and abolished protection of SDF-1β in T2D mice. Klf15-cKO and WT mice were subjected to the same treatment, as described in Fig. 4. The expression of KLF15 and CTGF were measured by western blotting assay (A). The expression of fibronectin and collagen I, TGF-β1 were examined by western blotting assay (B). Data are presented as mean ± SD (n = 6 at least in each group). Ctrl, control; T2D, type 2 diabetes; *, P < 0.05 vs. control group; #, P < 0.05 vs. T2D group; $, P < 0.05 vs. Klf15-cKO group.

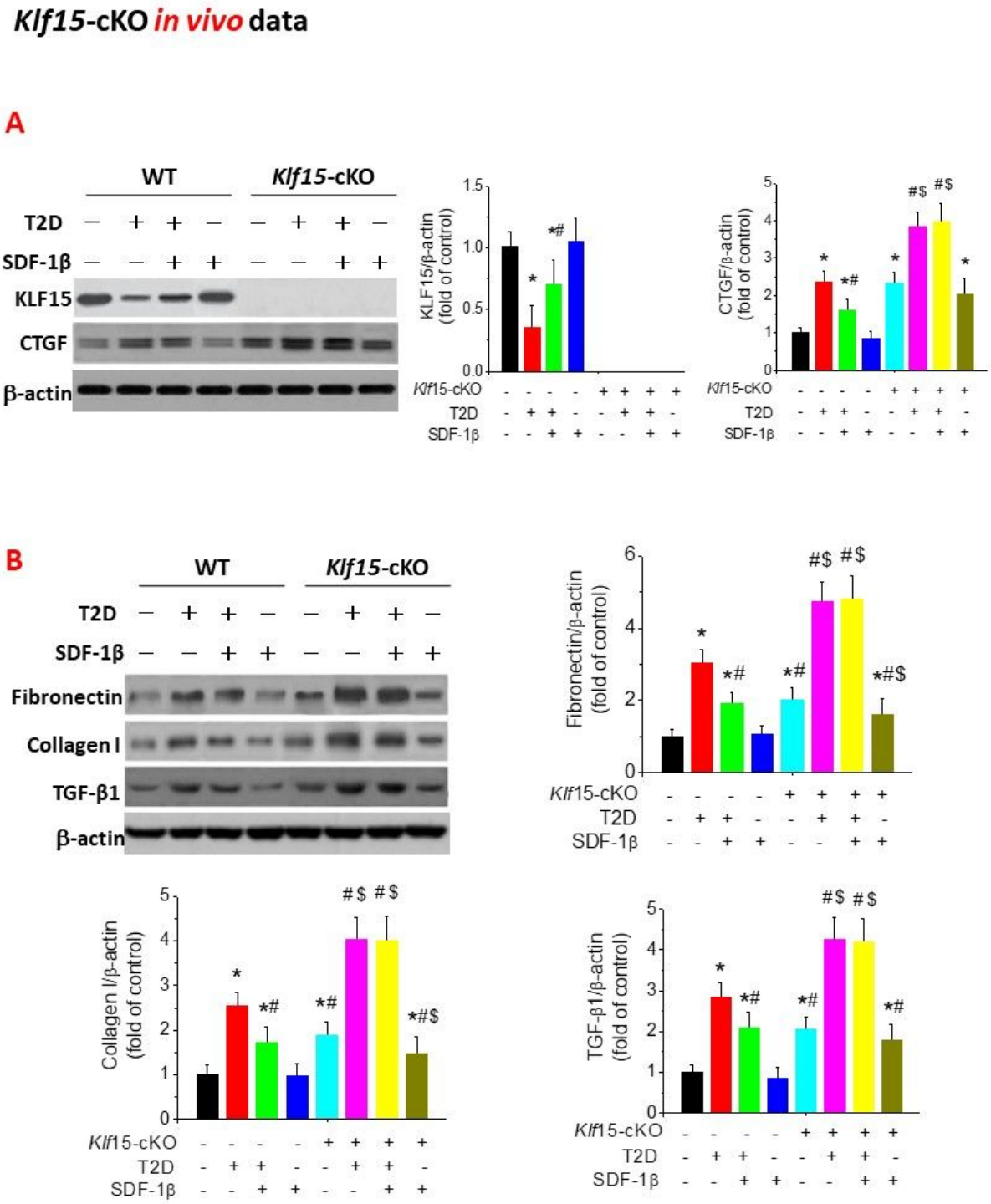

Fig. 5

Figure 5

Klf15-cKO aggravated the cardiac fibrosis and abolished protection of SDF-1β in T2D mice. Klf15-cKO and WT mice were subjected to the same treatment, as described in Fig. 4. The expression of KLF15 and CTGF were measured by western blotting assay (A). The expression of fibronectin and collagen I, TGF-β1 were examined by western blotting assay (B). Data are presented as mean ± SD (n = 6 at least in each group). Ctrl, control; T2D, type 2 diabetes; *, P < 0.05 vs. control group; #, P < 0.05 vs. T2D group; $, P < 0.05 vs. Klf15-cKO group.

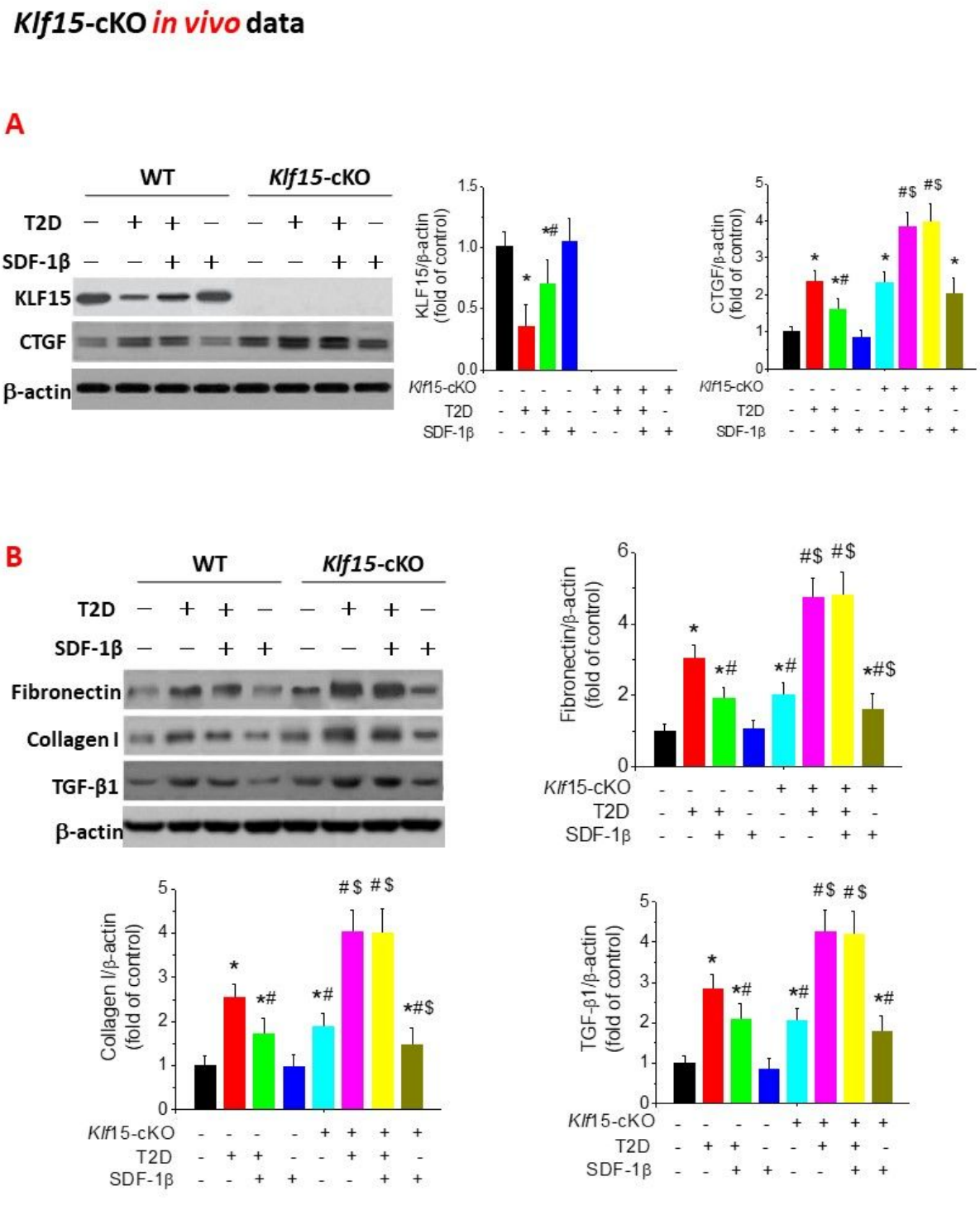

Fig. 5

Figure 5

Klf15-cKO aggravated the cardiac fibrosis and abolished protection of SDF-1β in T2D mice. Klf15-cKO and WT mice were subjected to the same treatment, as described in Fig. 4. The expression of KLF15 and CTGF were measured by western blotting assay (A). The expression of fibronectin and collagen I, TGF-β1 were examined by western blotting assay (B). Data are presented as mean ± SD (n = 6 at least in each group). Ctrl, control; T2D, type 2 diabetes; *, P < 0.05 vs. control group; #, P < 0.05 vs. T2D group; $, P < 0.05 vs. Klf15-cKO group.

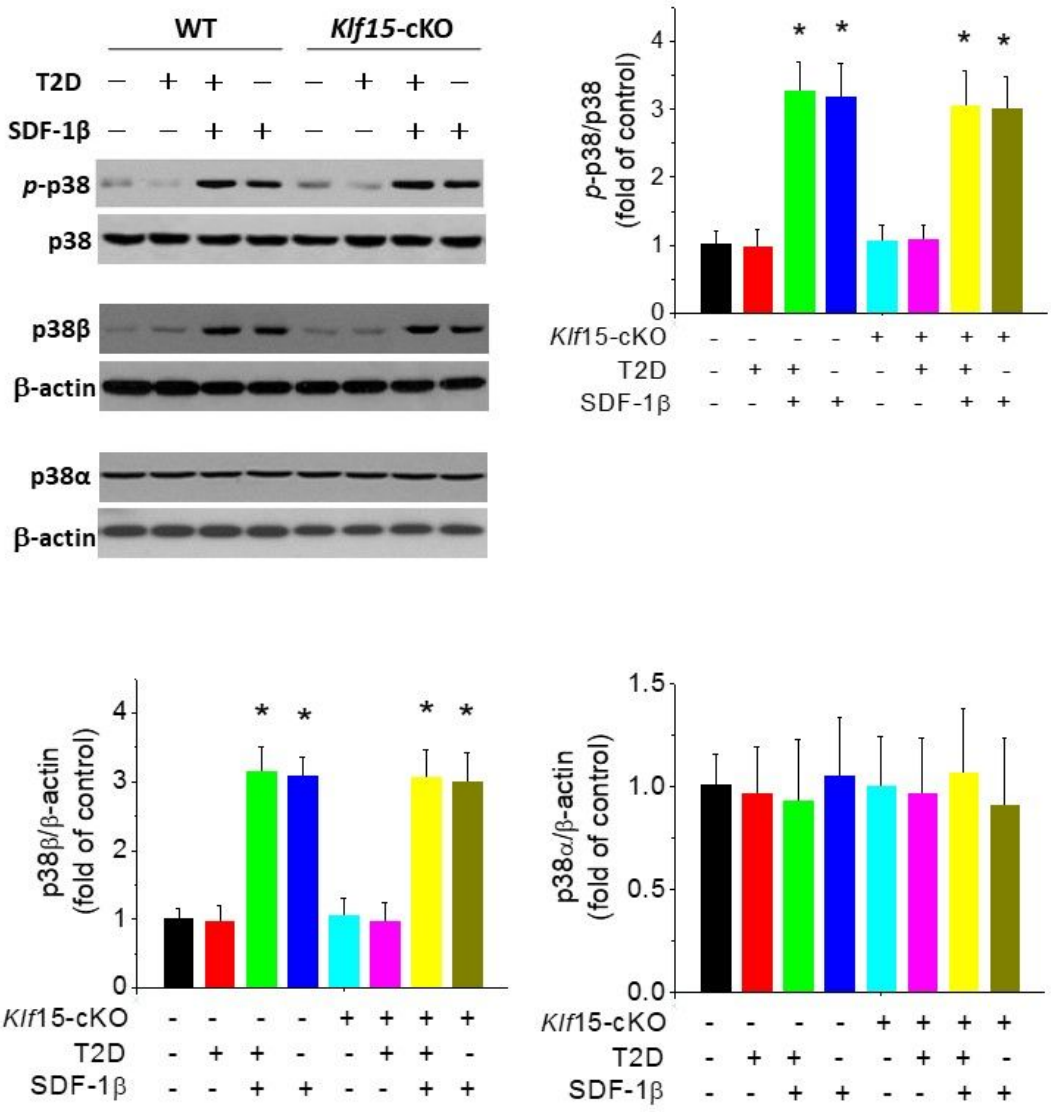

Fig. 6

Figure 6

Protective effect of SDF-1β on T2D-induced cardiac fibrosis is mediated by p38β MAPK up-regulation. Klf15-cKO and WT mice were subjected to the same treatment, as described in Fig. 4. The protein level of p-p38 MAPK, p38 MAPK, p38α MAPK and p38β MAPK in the cardiac tissues were examined by western blotting assay. Data are presented as mean ± SD (n = 6 at least in each group). Ctrl, control; T2D, type 2 diabetes; *, P < 0.05 vs. control group; #, P < 0.05 vs. T2D group; $, P < 0.05 vs. Klf15-cKO group.

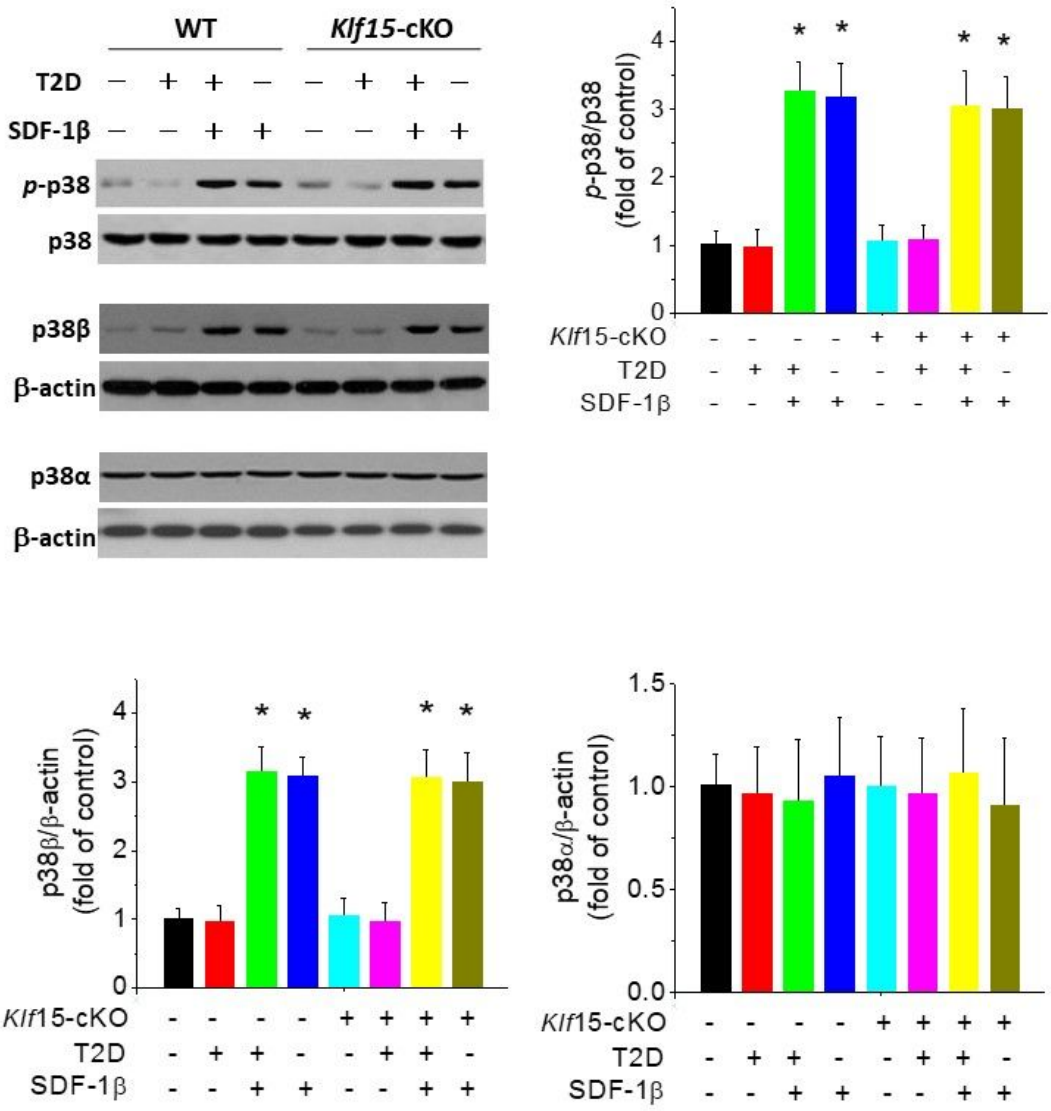

Fig. 6

Figure 6

Protective effect of SDF-1β on T2D-induced cardiac fibrosis is mediated by p38β MAPK up-regulation. Klf15-cKO and WT mice were subjected to the same treatment, as described in Fig. 4. The protein level of p-p38 MAPK, p38 MAPK, p38α MAPK and p38β MAPK in the cardiac tissues were examined by western blotting assay. Data are presented as mean ± SD (n = 6 at least in each group). Ctrl, control; T2D, type 2 diabetes; *, P < 0.05 vs. control group; #, P < 0.05 vs. T2D group; $, P < 0.05 vs. Klf15-cKO group.

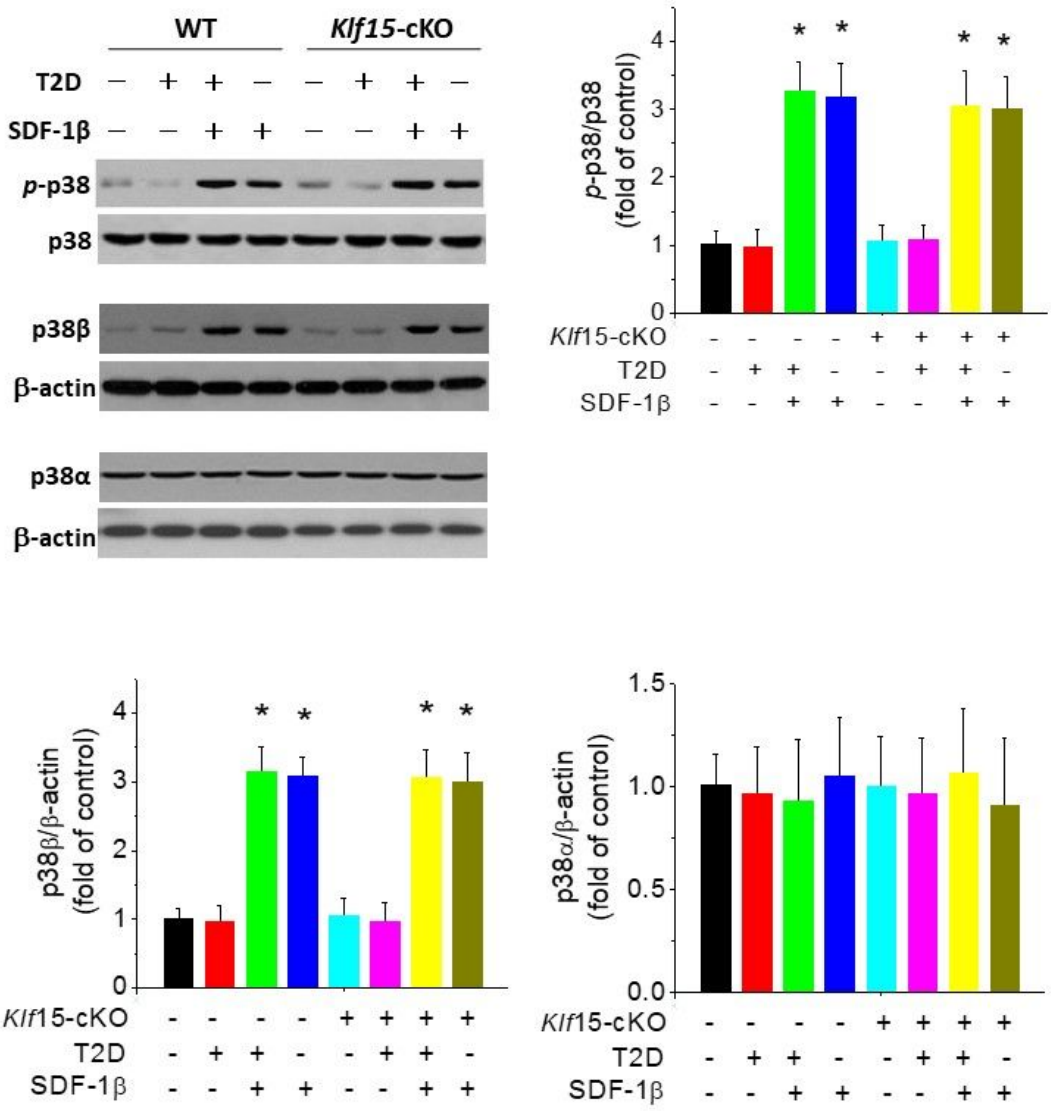

Fig. 6

Figure 6

Protective effect of SDF-1β on T2D-induced cardiac fibrosis is mediated by p38β MAPK up-regulation. Klf15-cKO and WT mice were subjected to the same treatment, as described in Fig. 4. The protein level of p-p38 MAPK, p38 MAPK, p38α MAPK and p38β MAPK in the cardiac tissues were examined by western blotting assay. Data are presented as mean ± SD (n = 6 at least in each group). Ctrl, control; T2D, type 2 diabetes; *, P < 0.05 vs. control group; #, P < 0.05 vs. T2D group; $, P < 0.05 vs. Klf15-cKO group.

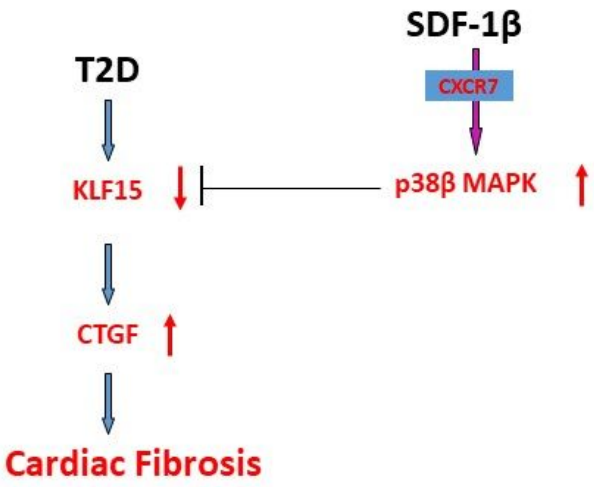

Fig. 7

Figure 7

Working hypothesis for the mechanism by which SDF-1β protects myocardium from T2D-induced fibrosis. The working hypothesis for the mechanisms underlying SDF-1β-induced attenuation of cardiac fibrosis in T2D mice are illustrated in schematic diagram.

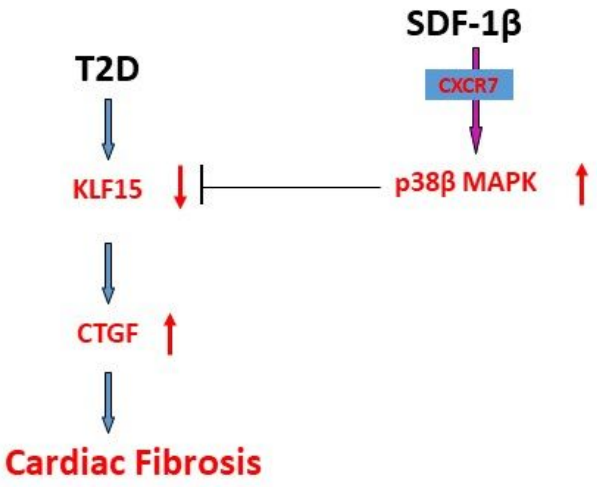

Fig. 7

Figure 7

Working hypothesis for the mechanism by which SDF-1β protects myocardium from T2D-induced fibrosis. The working hypothesis for the mechanisms underlying SDF-1β-induced attenuation of cardiac

fibrosis in T2D mice are illustrated in schematic diagram.

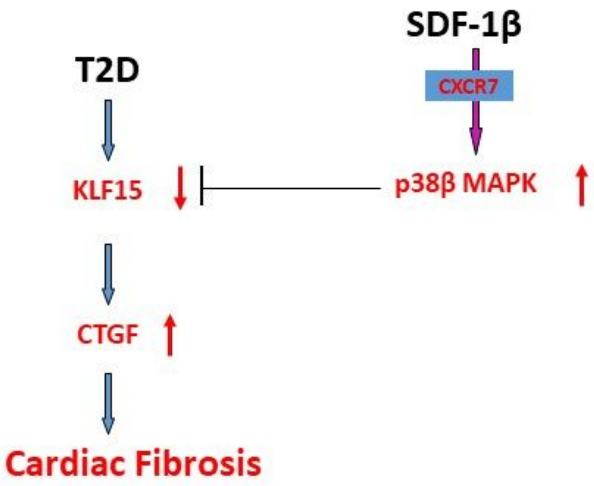

Fig. 7

Figure 7

Working hypothesis for the mechanism by which SDF-1β protects myocardium from T2D-induced fibrosis. The working hypothesis for the mechanisms underlying SDF-1β-induced attenuation of cardiac fibrosis in T2D mice are illustrated in schematic diagram.